Johanna Lyytikäinen

INTERACTION AND BARRIER PROPERTIES OF NANOCELLULOSE AND HYDROPHOBICALLY MODIFIED ETHYL(HYDROXYETHYL)CELLULOSE FILMS AND COATINGS

ACTA UNIVERSITATIS LAPPEENRANTAENSIS 955

Johanna Lyytikäinen

INTERACTION AND BARRIER PROPERTIES OF NANOCELLULOSE AND HYDROPHOBICALLY MODIFIED ETHYL(HYDROXYETHYL)CELLULOSE FILMS AND COATINGS

Dissertation for the degree of Doctor of Science (Technology) to be presented with due permission for public examination and criticism in the Auditorium 1316 at Lappeenranta-Lahti University of Technology LUT, Lappeenranta, Finland on the 31st of March, 2021, at 11 a.m.

Acta Universitatis
Lappeenrantaensis 955

Supervisor Docent Kaj Backfolk
LUT School of Energy Systems
Lappeenranta-Lahti University of Technology LUT
Finland

Reviewers Professor Per Engstrand
Department of Chemical Engineering
Mid Sweden University
Sweden

Professor Jouko Peltonen
Laboratory of Molecular Science and Engineering
Åbo Akademi University
Finland

Opponent Professor Jouko Peltonen
Laboratory of Molecular Science and Engineering
Åbo Akademi University
Finland

ISBN 978-952-335-638-2
ISBN 978-952-335-639-9 (PDF)
ISSN-L 1456-4491
ISSN 1456-4491

Lappeenranta-Lahti University of Technology LUT
LUT University Press 2021

Abstract

Johanna Lyytikäinen
Interaction and barrier properties of nanocellulose and hydrophobically modified ethyl(hydroxyethyl)cellulose films and coatings
Lappeenranta 2021
77 pages
Acta Universitatis Lappeenrantaensis 955
Diss. Lappeenranta-Lahti University of Technology LUT
ISBN 978-952-335-638-2, ISBN 978-952-335-639-9 (PDF), ISSN-L 1456-4491, ISSN 1456-4491

In food packaging applications, the oxygen barrier and resistance to oil and grease are essential properties of the packaging. The barrier performance of fibre-based packages needs to be improved with a coating, which is typically a fossil-based plastic. However, the demand for packaging made from more sustainable sources has been driving the development of bio-based coatings and especially of cellulosic materials for barrier materials.

Coatings and films consisting of methyl nanocellulose, hydrophobically modified ethyl(hydroxyethyl)cellulose (EHEC) and microfibrillated cellulose (MFC) were prepared. The temperature dependence and the interaction between the components in solution were investigated with rheological measurements. The film formation and barrier properties of the self-supporting films and coatings were investigated with surface imaging, wetting and liquid spreading and surface energy measurements and by measuring the oxygen transmission rate and the oil and grease resistance of the materials. The paperboard substrates were blade-coated but foam coating was also used to create thin coating layers on paper prepared with different levels of smoothness and hydrophobicity or hydrophilicity.

The interaction between the components was observed as changes in initial viscosity and in cloud point and gelation temperature, but also in the transparency of the films and in the oxygen barrier properties. In some cases, at elevated temperatures, air bubbles were formed in the cast films, but the air bubbles did not affect the oxygen transmission rate through the films. Cast films and methyl nanocellulose-based coatings were found to have a high resistance to oil and grease, but the spreading of the oil on the samples varied significantly suggesting that methyl nanocellulose and hydrophobically modified EHEC change the wettability of the surface. Even the low coat weights achieved with foam coating were able to make the surface more hydrophobic or to increase the oil repellence.

Creasing and folding of the coated substrates reduced the oil and grease resistance, but the addition of MFC to the coating composition seemed to improve the ability of the coating to resist cracking during converting. Post-drying of the methyl nanocellulose coating and conditioning of the methyl nanocellulose-EHEC coating at high relative humidity did not reduce the oil and grease resistance.

Keywords: coating, film formation, foam, oil and grease resistance, oxygen barrier

Acknowledgements

This work was carried out at Lappeenranta-Lahti University of Technology LUT between 2016 and 2020. This work has received financial support from Stora Enso Oyj and is gratefully acknowledged.

I would like to express my gratitude to my supervisor, Docent Kaj Backfolk for the guidance, discussions and support during this work. Professor Per Engstrand and Professor Jouko Peltonen are acknowledged for pre-examining the thesis.

Lic. Tech. Isto Heiskanen is thanked for co-operation and valuable comments. The co-authors are thanked for their help and valuable contribution to the publications. Dr. Anthony Bristow is thanked for the linguistic reviews of the papers and the thesis.

I would also like to thank my current and former colleagues. Especially Salla Hiltunen, Krista Koljonen, Teija Laukala, Katja Lyytikäinen and Sami-Seppo Ovaska are thanked for their help and valuable discussions during these years.

Finally, I am deeply grateful to my family for all the help and support I have received.

Johanna Lyytikäinen
February 2021
Lappeenranta, Finland

Contents

List of publications

This dissertation is based on the following papers. The rights have been granted by publishers to include the papers in dissertation.

I. Lyytikäinen, J., Laukala, T., and Backfolk, K. (2019). Temperature-dependent interactions between hydrophobically modified ethyl(hydroxyethyl)cellulose and methyl nanocellulose. *Cellulose*, 26(12), pp. 7079-7087.

II. Lyytikäinen, J., Morits, M., Österberg, M., Heiskanen, I., and Backfolk, K. (2021). Skin and bubble formation in films made of methyl nanocellulose, hydrophobically modified ethyl(hydroxyethyl)cellulose and microfibrillated cellulose. *Cellulose*, 28(2), pp. 787-797.

III. Lyytikäinen, J., Ovaska, S.-S., Heiskanen, I., and Backfolk, K. (2021). The role of MFC and hydrophobically modified ethyl(hydroxyethyl)cellulose in film formation and the barrier properties of methyl nanocellulose film. *Nordic Pulp & Paper Research Journal*. Accepted for publication.

IV. Lyytikäinen, J., Ovaska, S.-S., Heiskanen, I., and Backfolk, K. (2021). Film formation and foamability of cellulose derivatives: Influence of co-binders and substrate properties on coating holdout. *BioResources*, 16(1), pp. 597-613.

Author's contribution

The author was the corresponding author in all the papers. The author planned the experiments and performed the experimental work, except for the particle size measurements in Paper I, the AFM measurements in Paper II, and the SEM measurements in Papers II, III and IV. The papers were written together with the co-authors.

Abbreviations

AKD	alkyl ketene dimer
CMC	carboxymethylcellulose
CNC	cellulose nanocrystals
CNF	cellulose nanofibril
EHEC	ethyl(hydroxyethyl)cellulose
HPMC	hydroxypropylmethylcellulose
MFC	microfibrillated cellulose
NFC	nanofibrillated cellulose
n.m.	not measured
OGR	oil and grease resistance
OTR	oxygen transmission rate
PFOA	perfluorooctanoic acid
PLA	polylactic acid
QNM	quantitative nanomechanical mapping
RH	relative humidity
SEM	scanning electron microscope
s.c.	solids content
TEMPO	2,2,6,6-tetramethylpiperidine-1-oxyl
WVTR	water vapor transmission rate
ÅAGWR	Åbo Akademi gravimetric water retention

1 Introduction

1.1 Background

Packaging materials are often coated to improve their ability to act as a barrier to the transmission of oxygen, water or liquids, water vapour and grease or to achieve a better substrate for printing. Plastics are often used for coating the paper or paperboard due to their low cost and good barrier properties (Hubbe et al. 2017; Helanto et al. 2019), but the environmental concerns and a shift towards a circular economy have been driving the development of new coating materials to replace the fossil-based coating materials.

Recently more bio-based polymers have been investigated for coating paper or paperboard and high oxygen barrier and grease resistance have been achieved in several studies. Cellulosic materials, such as nano- or microfibrillated cellulose (NFC, MFC), have been studied as barrier materials due to the dense network which they form during dewatering and drying (Syverud and Stenius 2009; Lavoine et al. 2012; Österberg et al. 2013). Due to its renewability, recyclability, strength and unique barrier properties, nanocellulose has been of interest in films and coatings in several studies. Biodegradability and compostability without the formation of harmful degradation products are also important features of nanocellulose coatings as a replacement for fossil-based plastics (Vikman et al. 2015; Hubbe et al. 2017). A nanocellulose or microfibrillated cellulose coating has been found to provide a high oxygen barrier under dry conditions, which is an important feature in food packaging applications. The practical applications, however, often require that the barrier properties do not deteriorate at high relative humidity, and this means that the sensitivity of the hydrophilic MFC to water must be reduced, for example by modification of the MFC or using different coating compositions (Aulin et al. 2010; Spence et al. 2011).

A barrier layer can be created by coating or by preparing a self-supporting film. Extrusion coating is mainly used with fossil-based plastics, and with polymers reinforced with nanocellulose, but dispersion coating enables more bio-based coating components to be used. Unmodified or modified MFC and NFC have been utilized alone or as components of films or of coating solutions to create a barrier layer (Aulin et al. 2010; Hult et al. 2010; Lavoine et al. 2013; Kumar et al. 2016), but the use of novel nanocellulose materials or their combinations with other cellulosic materials as coating components have been less studied.

Recently, interest in foam forming in papermaking has increased and the use of MFC in foam coating has also been investigated (Kenttä et al. 2014; Kinnunen-Raudaskoski et al. 2014; Korehei et al. 2016; Kinnunen-Raudaskoski et al. 2017; Koponen et al. 2018). In general, foam coating is a method where a gas acts as a carrier for the coating material and transfers it between the bubbles onto the substrate (Kinnunen-Raudaskoski et al. 2014) and reduces the wetting of the substrate (Anderson 1977).

1.2 Objective of the study

Nanocellulose films and coatings can provide good barrier properties, but they often require the use of process or performance additives to be able, for example, to improve the stability and runnability of high-speed processes. As a consequence, the effect on the end product performance of such additives and of possible defects or for example the intentional or unintentional entrapment of air in the coating solutions or coatings must be clarified.

The aim of the work described in this thesis was to investigate cellulose-based, two-component formulations consisting of methyl nanocellulose, hydrophobically modified ethyl(hydroxyethyl)cellulose (EHEC) or native MFC. The modified nanocellulose or hydrophobically modified EHEC could have a good compatibility with MFC, but there may also be a temperature-dependent effect which could affect the process and the properties of the end product.

The role of additives and the temperature-sensitivity of the coating solutions and film formation were investigated. The interaction between the components and their temperature dependence were studied by determining the rheological properties of the solutions as a function of temperature, and the effect of concentration on the rheological properties of the pure solutions was also studied. The effect of the nanocellulose and cellulose derivatives on the foaming and foam properties were studied with viscosity, gravimetric water retention and foam stability measurements.

Cast films were prepared from the components in different ratios and dried at different temperatures in order to evaluate the effect of drying on the film formation and barrier properties. Solutions consisting of methyl nanocellulose, hydrophobically modified EHEC and MFC were prepared in order to clarify the role of additives in the coating composition on the film-forming and barrier properties. In addition, the role of using foam coating in creating thin coating layers on the substrate was evaluated. The mechanical durability and the role of co-additives in coatings subjected to creasing and folding was also studied. The film-formation was evaluated with scanning electron microscope (SEM), contact angle and barrier measurements.

2 Microfibrillated cellulose

Cellulose nanomaterials are renewable and sustainable materials produced by the disintegration of fibres into micro- or nanoscale dimensions. Depending on the preparation and pretreatment methods, microfibrillated cellulose can have diameter in both nanoscale and microscale (< 10 µm). Its rheological, strength and film-forming properties enable MFC to be used as reinforcement materials in composites or packaging materials, and in coatings and films. (Siró and Plackett 2010; Lavoine et al. 2012; Osong et al. 2016, Ciftci et al. 2020).

2.1 Native microfibrillated cellulose

During the preparation of MFC, cellulose fibres are disintegrated into smaller dimensions, but MFC has relatively wide size distribution (Ciftci et al. 2020). Figure 2.1. shows the dimensions and fibrillar structure of the MFC and fibre fragments.

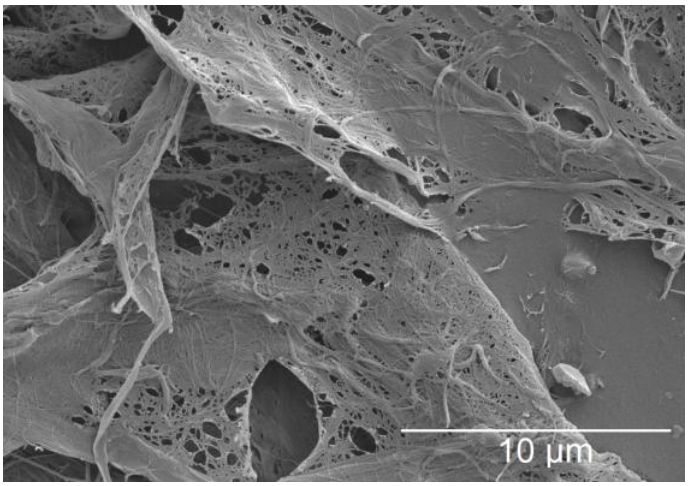

Figure 2.1: Microfibrillated cellulose and fibre fragments.

The reduction in particle size in the preparation of MFC leads to an increase in the viscosity of the fibre suspension. MFC forms a highly viscous gel already at low concentrations, due to the strong network formed as a result of entanglements between the fibrils in the MFC suspension (Pääkkö et al. 2007). An MFC suspension is shear-thinning, due to the breakdown of the flocs under shear so that the individual fibres become orientated in the flow direction leading to a decrease in viscosity. A small peak in the viscosity curve at shear rates between 10 and 100 s^{-1} is a common feature of a MFC suspension, and it has been suggested that this is due to an increase in the floc size and size distribution (Iotti et al. 2011; Karppinen et al. 2012; Hiltunen et al. 2018). At shear rates above 100 000 s^{-1}, a 1 wt-% MFC suspension has shown dilatant behaviour and this

limits its utilization for high shear coating applications (Lavoine et al. 2012). The rheological behaviour of an MFC suspension is affected, for example, by the dimension of the fibrils, the solids content and the temperature (Pääkkö et al. 2007; Iotti et al. 2011).

MFC has a high specific surface area and a high aspect ratio (Xhanari et al. 2011). The large specific surface area increases its ability to form hydrogen bonds and this, with the high aspect ratio, increases its strength properties (Pääkkö et al. 2007; Nair et al. 2014). In addition, its high water retention capacity has been attributed to the large specific surface area and plays an important role for example in coating processes. The water-holding capacity of MFC when a suspension at low concentration is applied to a substrate requires a high drying capacity. Achieving an adequate and uniform coating layer is challenging due to the high viscosity and high water retention properties of MFC at low concentrations. (Lavoine et al. 2012; Kumar et al. 2014).

The crystallinity of MFC is relatively high, and this is beneficial for its barrier-forming properties. The dense network and the crystalline regions of MFC hinder the penetration of molecules such as oxygen through the MFC film (Syverud and Stenius 2009; Lavoine et al. 2012; Österberg et al. 2013), although the barrier properties may be affected by pores formed in the film between the fibrils during drying (Aulin et al. 2010; Lavoine et al. 2012).

Due to the hydrophilic character of cellulose, MFC is sensitive to water, and the cellulose network in the MFC film is loosened at higher relative humidities due to a weakening of the hydrogen bonds leading to a deterioration in the barrier properties. (Herrera et al. 2017; Solala et al. 2018). In addition, the amorphous regions in cellulose absorb water and the water vapour transmission rate (WVTR) of the MFC film is high (Aulin et al. 2010; Tammelin et al. 2015) and MFC is therefore a poor or only moderate water vapour barrier. An increase in the degree of crystallinity can improve the barrier properties at a higher relative humidity, since the crystalline regions are impermeable to water. (Herrera et al. 2017; Solala et al. 2018). In practical applications, the material must preserve its barrier properties at high relative humidities, and this requires a modification of the cellulosic materials.

2.2 Modified microfibrillated cellulose

To increase the fibrillation and enhance the barrier properties, a pre-treatment with e.g. TEMPO (2,2,6,6-tetramethylpiperidine-1-oxyl)-oxidation (Fukuzumi et al. 2009) or carboxymethylation (Aulin et al. 2010; Minelli et al. 2010) can be used. In addition, cross-linking (Herrera et al. 2017), the use of a coating or filler (Spence et al. 2011) or post-curing have been proposed for the modification of MFC.

In TEMPO-mediated oxidation, the surface of the cellulose is modified, and the crystallinity of the material remains unchanged. This leads to a smaller fibril diameter compared to native MFC and the films prepared from TEMPO-oxidized MFC are transparent and enhance the gas barrier of the MFC films. (Fukuzumi et al. 2009; Lavoine

et al. 2012), although the wettability of the TEMPO-oxidized MFC is increased. The adsorption of a cationic surfactant on the TEMPO-mediated oxidized nanofibrils or treating the TEMPO-oxidized film with a cationic alkyl ketene dimer has been found to increase the hydrophobicity and thus reduce the wettability (Fukuzumi et al. 2009; Isogai et al. 2011; Xhanari et al. 2011).

The hydrophobicity of MFC can be increased through a surface modification such as esterification, where hydrophobic moieties are introduced into the hydroxyl groups in the surface and crystalline regions remain unchanged. (Rodionova et al. 2011; Rodionova et al. 2013; Sehaqui et al. 2013; Vuoti et al. 2013). The hydrophobization affects the water absorption of the MFC film more than the WVTR value. This can be seen for example as an increase in the contact angle of water or as a reduction in the water uptake. Some increase in pore size can be observed after hydrophobic modification and the pore volume in the film probably affects the WVTR value. (Rodionova et al. 2011; Sehaqui et al. 2013; Solala et al. 2018). The surface modification can also create a better compatibility with non-polar polymers and thus the ability to use MFC as a reinforcement in composites (Andersen et al. 2006; Rodionova et al. 2011).

2.2.1 **Methyl nanocellulose**

Methylcellulose is known as a thermoresponsive cellulose derivative, showing a reduced solubility and gelation at elevated temperatures, although it is soluble in water at lower temperatures (Kamitakahara et al. 2008; Arvidson et al. 2013).

Methyl nanocellulose is a water-soluble amphiphilic polymer and can be prepared from methylcellulose through a cleavage process. The methyl nanocellulose has a low viscosity and small particle size (particle diameter 250 nm). It also has a low surface tension and thus forms foam and could be used as a surfactant (Jin 2017; Innotech Materials).

3 Thermoresponsive cellulose derivatives

The solubility of cellulose in water can be modified through derivatization, where the structure of the hydroxyl groups of cellulose is chemically modified. Modification with hydrophilic functional groups increases the solubility of cellulose whereas the introduction of hydrophobic groups can be used to adjust, for example, intra and intermolecular associations and temperature dependence. The solubility of many cellulose derivatives decreases with increasing temperature due to hydrophobic groups in the polymer, and because polymer-polymer interactions via hydrophobic groups become favourable due to the increase in temperature. Derivatization can also be utilized to modify the strength and barrier properties of films and the rheological properties of the solutions. (Karlson et al. 2000; Jain et al. 2013; Paunonen 2013).

Water-soluble cellulose derivates such as carboxymethylcellulose (CMC), hydroxypropyl cellulose, methylcellulose and ethyl(hydroxyethyl)cellulose (EHEC) can be utilized in various applications such as surfactants, and in food and paints as emulsion-stabilizers and rheology-modifiers. Methylcellulose and hydrophobically modified EHEC have an amphiphilic character, containing both hydrophilic and hydrophobic groups, which give them surfactant-like properties. Surface-active polymers orientate in a manner similar to that of surfactants, where the hydrophilic parts of the polymer are towards the water and the hydrophobic parts away from the water and they are thus able to increase the stability of dispersed systems. Hydrophobically modified EHEC is effective already at low concentrations since the polymer adheres to interfaces and surfaces. (Karlson et al. 2000; Wei et al. 2008; Jain et al. 2013; Kronberg et al. 2014). Cellulose is also considered to be an amphiphilic polymer due to its high hydrophilicity and its insolubility in water due to internal hydrogen bonding (Lindman et al. 2010).

3.1 Methylcellulose

Methylcellulose has been used widely in pharmaceutical and food applications due to its ability to form a transparent and flexible film with a good barrier to lipids and oxygen (Fairglouch et al. 2012; Jain et al. 2013). The solubility of the thermoresponsive methylcellulose in water is high at low temperatures, but it forms a gel at elevated temperatures. Methylcellulose has an uneven distribution of methyl groups and thus contains both hydrophilic and hydrophobic parts. The degree of substitution affects the solubility. The hydrophilic parts enhance the solubility in water, but at elevated temperatures, association occurs between hydrophobic groups, leading to a gelation of the methylcellulose solution. (Kamitakahara et al. 2008; Arvidson et al. 2013; Jain et al. 2013).

Gelation at elevated temperatures is characteristic of methylcellulose and there are a few hypotheses describing the mechanism of gel formation. At lower temperatures, the water molecules surround the polymer in aqueous solution, but at elevated temperatures the

hydrogen bonds are weakened, and this facilitates the association of hydrophobic methyl groups in the polymer to form a network (Fairclough et al. 2012; Arvidson et al. 2013).

3.2 Ethyl(hydroxyethyl)cellulose

Ethyl(hydroxyethyl)cellulose (EHEC) is a nonionic cellulose derivative. An aqueous EHEC solution starts to separate into two phases, polymer-rich and polymer-poor, and becomes cloudy when it is heated to a certain temperature, referred to as the cloud point. Clouding of the EHEC solution is due to the intermolecular association via small amounts of hydrophobic groups in the EHEC polymer. (Carlsson et al. 1986; Nyström et al. 1995; Thuresson and Lindman 1997).

The EHEC and anionic surfactant interact via hydrophobic groups and this affects the rheological behaviour of the solution. The amount of surfactant and surfactant type added to the EHEC solution and solids content of the solution affect the rheological properties. The addition of surfactant is known to increase the viscosity upon heating and this thermoreversible gelation leads to the formation of a transparent gel (Nyström et al. 1996; Thuresson and Lindman 1997; Wang et al.1997). The interaction between the surfactant and EHEC can be characterized by e.g. viscosity, oscillatory and cloud point measurements (Nyström et al. 1995; Thuresson and Lindman 1997; Kjøniksen et al. 1998).

3.3 Hydrophobically modified ethyl(hydroxyethyl)cellulose

Water-soluble cellulose derivatives can be modified to achieve different degrees of hydrophobicity. To increase the hydrophobicity of EHEC, hydrophobic side groups can be grafted to the EHEC backbone. The length of the hydrophobic group affects the cloud point of the hydrophobically modified EHEC, since the association occurs via hydrophobic groups and the cloud point is reduced with an increasing hydrophobicity. As a result of the hydrophobic modification, the viscosity increases due to its self-associative behaviour through the hydrophobic parts, especially at elevated temperatures (Thuresson and Lindman 1997; Karlson et al. 2000). The increase in viscosity is evident in dilute solutions since the network is formed already at low concentrations, but the association is weak and the flocs are broken easily, so that the viscosity decreases when the solution is sheared (Kronberg et al. 2014).

4 Interactions in polymer and nanocellulose solutions

The use of MFC and NFC as reinforcement in both biodegradable and non-biodegradable composites and blends has shown a growing interest. The tendency for native MFC or NFC to form hydrogen bonds between fibrils gives the MFC or NFC film its strength properties (Siró and Plackett 2010), although the hydrophilicity restricts its compatibility with non-polar components (Wang et al. 2018). Modification of MFC or NFC improves the compatibility, but this can cause a weakening of the strength properties of the fibrils (Eronen et al. 2011).

4.1 Association and adsorption

The phase behaviour of two polymers in aqueous solution depends on the interaction between the polymers. Hydrophobically modified cellulose derivatives are associative and they can form either intramolecular or intermolecular bonds. Intramolecular association occurs mostly at low concentrations. Intermolecular association occurs between molecules and creates a network and is probably the cause of the increase in viscosity, although the degree of substitution and the distribution of the hydrophobic groups in the polymer also affect the viscosity. (Winnik and Yekta 1997; Karlson et al. 2000). The polymer-MFC interaction in a non- polar polymer matrix is weak due to the hydrophilic nature of MFC but it can be enhanced for example by the surface modification of MFC or by the addition of a surfactant (Salas et al. 2014).

Phase separation can occur in a polymer solution as either an associative or a segregative phase separation. An associative phase separation occurs when there are strong attractive forces between polymers of opposite charge and this type of phase separation can also be observed with hydrophobic polymers, especially at elevated temperatures. (Kronberg et al. 2014). A segregative phase separation is an undesirable phenomenon and is typical for non-aqueous solutions but is also observed with nonionic polymers in water. When there are repulsive forces between two polymers, the solution containing the polymers separates into two phases, one containing one of the polymer and the other containing the other polymer. For example, hydrophobically modified EHEC and its unmodified analogue in aqueous solution do not associate and they show this kind of phase separation. (Thuresson and Lindman 1997; Nilsson et al. 2000).

The interaction between EHEC or hydrophobically modified EHEC and surfactants and its effect on phase behaviour has been studied widely. Surfactants are adsorbed onto the hydrophobic parts of EHEC, and the association between EHEC and an anionic surfactant leads to an increase in viscosity, since the association between polymer chains becomes stronger. The cloud point temperature increases when the surfactant binding to the polymer is high, and less surfactant binding is observed as a reduction in cloud point temperature. The addition of a large amount of surfactant to the solution breaks the intermolecular bonds, and intramolecular associations are formed, which is evident as a

decrease in the viscosity. (Thuresson et al. 1995; Thuresson and Lindman 1997; Olsson et al. 2005).

4.1.1 Adsorption onto solid surfaces and association in solutions

It has been suggested that the interaction between cellulose derivatives and native nanocellulose occurs via hydrophilic groups, or via hydrophobic groups in the case of the amphiphilic native cellulose (Eronen et al. 2011). The interaction via hydrophilic groups requires an uneven distribution of substituted groups on the cellulose derivative in order to achieve an adsorption of cellulose derivative onto the cellulose (Sundman 2014). This kind of interaction has been suggested to occur between hydroxypropyl methylcellulose (HPMC) and cellulose whiskers or MFC (Bilbao-Sainz et al. 2011; Larsson et al. 2012) and methylcellulose and cellulose nanocrystals or nanocellulose (Khan et al. 2010; McKee et al. 2014). However, the hydrogen bonding has been questioned especially in the case of methylcellulose. The interaction was affected by the surface morphology, the substituent type and the degree of substitution when the adsorption of cellulose derivatives onto cellulose surfaces was investigated. (Sundman 2014). In addition, the binding between hydroxypropyl methylcellulose and MFC was found to lead to a decrease in permeability of the films, and it was suggested that HPMC may gel and block the pores in the MFC film (Larsson et al. 2012).

4.1.2 Effects of pH, salt and polymer concentration on the interaction

The interaction between flocs in the MFC suspension decreases at a high pH and the network structure is loosened, which can be seen as a decrease in viscosity under low shear (Saarikoski et al. 2015). The addition of carboxymethylcellulose to cellulose nanofibrils in aqueous solution reduces the interaction between the fibrils and breaks up the fibril flocs, leading to fibril orientation and a reduction in both loss and storage moduli (Pahimanolis et al. 2013).

Electrolyte concentration and the type of electrolyte are known to influence the properties in solution of both nanocellulose and amphiphilic polymers. In the case of an amphiphilic polymer, both anionic and cationic ions influence the solution properties and cloud point. When phase separation occurs, the polymer phase has the higher salt content. The effect of an electrolyte depends on the electrolyte type. For example, sodium chloride (NaCl) in the solution makes it more polar and facilitates phase separation. The bonding between water and salt increases and the hydrophobic interactions in the polymer thus become stronger. This is observed as a decrease in the gelation and cloud point temperatures. (Carlsson et al. 1986; Nyström et al. 1996; Xu et al. 2004; Khuman et al. 2014).

The concentration of polymer affects the gelation and cloud point temperatures of methylcellulose and hydrophobically modified EHEC. In general, this is due to a greater number of molecules in the solution, which are closer to each other and able to more easily interact via hydrophobic groups, when the temperature increases. In the case of surfactant, its concentration in the polymer solution also affects the cloud point.

(Arvidson et al. 2012; Nyström et al. 1996). The addition of cellulose nanocrystals at different amounts to methylcellulose has also been found to increase the gel stiffness (McKee et al. 2014).

4.1.3 Effect of temperature on the interaction

In general, the solubility of a polymer in a solvent increases as the temperature increases, but for nonionic polymers the opposite behaviour is observed. It is suggested that the water molecules surround the hydrophobic groups in aqueous solution, and when the solution is heated, the association of the hydrophobic groups is enhanced due to the weakening of the hydrogen bonding. The polymers are thus able to form intermolecular bonds which results in network formation and becomes evident as an increase in viscosity. (Karlson et al. 2000; Fairclough et al. 2012; Arvidson et al. 2013). The amount of data available regarding the effect of temperature on the interaction between polymers and nanocellulose is limited, but the gel stiffness has been found to increase with the addition of cellulose nanocrystals and this effect was greater at elevated temperatures (McKee et al. 2014). In the case of MFC, the viscosity of the MFC suspension decreases at elevated temperature. The swelling of the fibrils is lower at elevated temperatures which leads to a higher mobility of the fibrils in the suspension. (Iotti et al. 2011).

Polymer solutions also show clouding at elevated temperatures at the point where the solution starts to separate into polymer-poor and polymer-rich phases, where the polymers start to form aggregates so that the solution is able to scatter light. (Fairclough et al. 2012). In addition, in the case of methylcellulose, for example, the gelation temperature depends strongly on the rate of heating and on the concentration. A slower heating rate leads to a lower gelation temperature. (Arvidson et al. 2013).

4.2 Foam and bubble formation and stability

In general, a foam can be defined as a dispersion of gas in a solid or liquid. Foam is formed in the presence of surface-active component. The surfactant reduces the surface tension and enables foaming and stabilizes the foam. The use of surfactants has, however, given rise to environmental concerns. The low biodegradability and aquatic toxicity of many surfactants have promoted the development of more bio-based and biodegradable surfactants (Kronberg et al. 2014; Lam et al. 2014; Fujisawa et al. 2017; Gong et al. 2017).

Alternative solutions for surfactants as stabilizing agents are amphiphilic polymeric surfactants. They have a tendency to attach to interfaces and to stabilize air bubbles and they can thus be utilized in foam formation. (Kronberg et al. 2014). Nanocelluloses can also act as Pickering stabilizers and they have been used, for example, in aerogels and foam-forming applications, where a system containing air bubbles or foam is prepared intentionally (Lam et al. 2014; Fujisawa et al. 2017).

Foams can be stabilized with small spherical particles which form a contact angle of 90° with the air-water interface. These particles attach well to the bubble surface, but in

practical applications, the contact angle is lower due to irregular shape and size and the packing of particles at the interface (Pugh 2016). The particle-stabilized foams are called Pickering foams. Pickering stabilization is usually related to highly stabilized emulsions, where relatively hydrophilic particles are adsorbed at oil-water interfaces, but the term ”Pickering stabilization” has recently been used to refer to the stabilization of air-water interfaces to create highly stable foams where partially hydrophobic particles are strongly attached to the air-water interface. In these particle-stabilized foams, the collapse and growth of the bubbles is reduced by the layer of particles at the air-water interface (Cervin et al. 2013; Lam et al. 2014; Fujisawa et al. 2017).

The stability of an aqueous foam can be increased by the addition of cellulose particles. The rod-like fibrils enhance the stability of the foam due to their ability to form entanglements around the bubble, thus providing more stable foams (Cervin et al. 2015). Native nanocellulose can for example be modified chemically, and polymers can be adsorbed onto native nanocellulose in order to increase the hydrophobicity and to create highly stable foams. Native and TEMPO-oxidized cellulose nanofibril foams have also been formed by adsorbing surfactants onto the surface of the nanofibrils (Cervin et al. 2013; Cervin et al. 2015; Cervin et al. 2016). Cellulose nanocrystals can be used to increase the stability of a methylcellulose foam, even at elevated temperatures (Hu et al. 2016). The structure of an MFC-based foam after freeze-drying is shown in Figure 4.1.

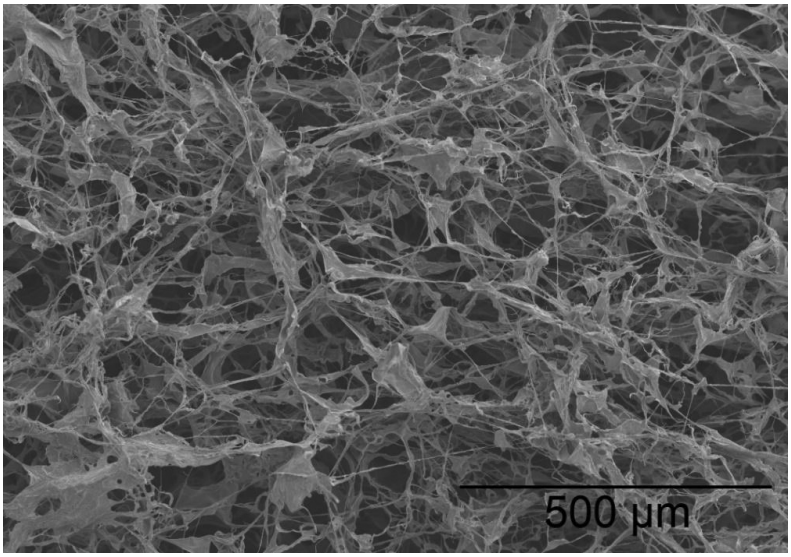

Figure 4.1: SEM micrograph of MFC-based foam after freeze-drying.

Interest in using nanocellulose in foams has been growing. Nanocellulose-based foams have a low density and are mechanically strong foams and are used in various applications, such as pharmaceutics, cosmetics and thermal insulation (Lavoine and Bergström 2017). Nanocellulose-based wet foams have been generated and stabilized

with the aid of surfactants. For example, TEMPO-oxidized cellulose nanofibrils can be foamed in the presence of surfactants and further stabilized with calcium ions (Gordeyeva et al. 2016). In addition, in the presence of retention aid and surfactant, MFC can increase the stability of pulp foams (Liu et al. 2018).

5 Film formation and end product properties of nanocellulose-based films and coatings

In food packaging, one of the main functions of the package is to protect the product from deterioration by oxygen or moisture. In addition, grease an oil resistance is an important requirement especially in fast food packaging. Fossil-based polymers are used to improve the barrier properties, but plastic-free packaging can be used for example for dry foods. Polyethylene provides a good liquid barrier, whereas poly(ethylene terephthalate) is used to provide an oxygen barrier (Paunonen 2013).

5.1 Film formation and temperature-dependence of films based on nanocellulose and cellulose derivatives

Nanocellulose films can be prepared by casting or filtration with properties that depend on the nanocellulose type and on the preparation method (Lavoine et al. 2012; Hubbe et al. 2017). Various drying conditions and strategies can be used when drying the films, but the nanocellulose films shrink during drying. The evaporation of water is faster from the film surface, and this, together with the slower evaporation of water from the nanocellulose itself, creates moisture gradients which create stresses in the films. Restrained drying has been found to reduce these increasing the fibril orientation and thus improving the mechanical properties of the films. (Baez et al. 2014). The aggregation of microfibrils occurs especially at higher temperatures, so that drying at room temperature and at 95 % relative humidity does not lead to the aggregation of the fibrils (Salmén and Stevanic 2018).

The drying conditions have also been found to affect the hydrophobicity of the methylcellulose films leading to an increase in crystallinity at higher temperatures and thus to a reduction in the water vapor permeability (Debeaufort et al. 2000; Cheng and Jones 2019). The higher temperatures may also affect the crystallinity of the nanocellulose, and for example an increase in crystallinity increases the oxygen barrier provided by the nanocellulose films (Helanto et al. 2019).

5.2 Strength and optical properties of nanocellulose films

Fibre-based materials are used in packaging due to their sustainability, light weight and strong mechanical properties. MFC can be used in packaging materials as a reinforcement agent, as a coating or in films. Nanocellulose increases the strength of paper or paperboard due to its high specific surface area and hydrogen-bonding ability. Films and coatings made of nanocellulose have been reported to have a high tensile strength and a high elastic modulus (Syverud and Stenius 2009). The mechanical properties of nanocellulose depend on the type of pre-treatment, which can affect the fibril size and thus the ability to form hydrogen bonds between the fibrils (Lavoine et al. 2012; Kumar et al. 2014). Cellulose nanocrystals form a more rigid and brittle film than microfibrillated cellulose due to their

smaller dimensions, and nanocellulose can improve the mechanical properties of films based on cellulose derivatives (Paunonen 2013), such as hydroxypropyl methylcellulose (Bilbao-Sainz et al. 2011), hydroxyethylcellulose (Sehaqui et al. 2011) and methylcellulose (Khan et al. 2010).

Many bio-based coating components such as starch make the coating brittle and the film-forming properties of bio-based coatings are often improved with a plasticizer (Hubbe et al. 2017). In packaging applications, the material should be able to resist stresses during creasing and folding in order to avoid cracking of the coating and delamination of the layers both in the coating and in the substrate (Beex and Peerlings 2009; Tanninen et al. 2015). MFC and CNF films have been found to withstand folding (Spence et al. 2010; Fein et al. 2020), but delamination may occur both in the substrate and between the coating and the substrate with an MFC or CNF coating. MFC- and CNF-coated paperboards have been found to have a higher tensile strength (Tayeb et al. 2020), and the coating also improves the resistance to folding and increases the bending stiffness (Lavoine et al. 2014). Folding of the CNF-coated material, however, leads to defects in the material even with a coat weight of 16 g/m^2, although the defects were found not to affect the grease resistance of the coated material (Tayeb et al. 2020).

Nanocellulose films can be highly transparent. The optical properties of nanocellulose are influenced by the dimensions of the nanocellulose, the aggregation of the fibres and the surface roughness (Nogi et al. 2009; Siró and Plackett 2010). The films are more transparent with small fibres, since large fibres scatter light. When blends of polymer are used, the transparency of the matrix can be retained if the different materials have similar refractive indices. In addition, the incompatibility of the materials can lead to air gaps or agglomeration which result in a more opaque film. (Hubbe et al. 2017).

5.3 Oxygen barrier

In general, the oxygen barrier properties of a material depend on the relative humidity, but a barrier is considered to be a moderate barrier if the oxygen transmission rate is between 6 and 100 ml/(m^2·day) (Khalifa 2016). The use of MFC as an oxygen barrier material has been demonstrated in several publications. MFC provides an oxygen barrier under dry conditions due to its crystallinity and its ability to form a dense network (Aulin et al. 2010). The dense network and polarity of the native MFC film hinder the penetration of gaseous molecules such as those of non-polar oxygen. The dense network has a high tortuosity, and gas diffusion through the MFC film is slow, although the pores between the fibrils formed during drying of the film allow gas to permeate through the film. If the film has no pores, the permeation depends on the diffusion and dissolution of the gas. The crystallinity also affects the barrier properties, but the high crystallinity of the cellulose nanocrystals does not necessarily lead to a good oxygen barrier due to the rigidity of the CNC particles which do not form a dense and nonporous network like the more flexible MFC or NFC. (Syverud and Stenius 2009; Nair et al. 2014; Ferrer et al. 2017). The reinforcement of cellulose derivatives with highly crystalline CNC gives a composite

material good water vapor barrier properties, and nanocellulose has also been used to reinforce cellulose derivatives in order to improve the mechanical and oxygen barrier properties (Paunonen 2013). Examples of the use of nanocellulose in various bio-based matrices and their measured barrier properties are presented in Table 5.1.

Table 5.1: MFC types in various bio-based matrices and their barrier properties.

MFC type	Matrix	Barrier	Ref.
MFC	PLA	Water vapour	1
MFC	Pullulan	Oxygen, water vapour	2
NFC	Arabinoxylan	Oxygen	3
MFC	Galactoglucomannan	Oxygen	4
Carboxymethylated MFC	Amylopectin	Oxygen	5
MFC	Amylopectin	Oxygen	5
Carboxymethylated CNF	Xylan	Oxygen, water vapour	6
NFC	CMC	Water vapour	7
NFC	HPMC	Water vapour	8
TEMPO-oxidized NFC	HPMC	Water vapour	8
Bacterial CNC	HPMC	Moisture	9
NFC	Methylcellulose + plasticizer	Water vapour	10

[1)] Sanchez-García et al. 2010 [2)] Cozzolino et al. 2014 [3)] Stevanic et al. 2012 [4)] Oinonen et al. 2016 [5)] Plackett et al. 2010 [6)] Hansen et al. 2012 [7)] Oun and Rhim 2015 [8)] Bilbao-Sáinz et al. 2011 [9)] George et al. 2014 [10)] Khan et al. 2010

5.4 Oil and grease resistance

Paper or paperboard materials are often used for food packaging, but the oil and grease resistance (OGR) of these materials is often not sufficient. Various techniques such as chemical modification and coating have been suggested to improve the oil and grease resistance of fibre-based packaging materials (Andersson 2008) and interest in sustainable greaseproof packaging materials has been growing significantly.

Cellulose films are good oil and grease barriers due to the weak interaction between non-polar grease or oil and the polar, hydrogen-bonded dense film structure of the cellulose, and the penetration of oil through the film is therefore slow (Aulin et al. 2010; Hubbe et al. 2017). Usually, lower surface energy increases the barrier to oil and grease migration. On the other hand, a polar component dissolves polar components and thus high polarity with high surface energy has also been shown to be beneficial for increasing the OGR (Ovaska et al. 2015; Sheng et al. 2019). The penetration time of grease and oil through the material is also affected by the amount of saturated and unsaturated fatty acids in the oil or grease (Helanto et al. 2019) and the oil sorption increases when the oil consists a greater amount of saturated fatty acids (Olafsson and Hildingsson 1995).

Surface treatment with fluorochemicals has been utilized to decrease the surface energy and improve the oil repellence, but the toxicity, low biodegradability and possible migration into food products of the fluorochemicals has increased interest in finding other ways of improving grease resistance (Aulin et al. 2010; Kisonen et al. 2014; D'Eon et al. 2009). The use of perfluorooctanoic acid (PFOA) and its related components have been restricted in applications where oil and grease resistance is required such as in food packaging applications (European Commission 2017).

Coating with more sustainable and bio-based polymers has also been used to improve the oil and grease resistance. In the case of a porous surface, the penetration of oil is due to capillary forces. Coating of the paper or paperboard densifies the surface and makes the surface notably non-porous and this prevents the oil from penetrating into the material (Aulin et al. 2010; Hult et al. 2010; Li et al. 2013). Grease penetration decreases when the coating thickness and uniformity increase, due to an increase in tortuosity in the coating. When the surface is closed, the air permeance is also decreased, and this has been found to correlate with the grease resistance (Kjellgren et al. 2006; Aulin et al. 2010; Zhong et al. 2019). Increasing the nanoscale roughness can also be used to increase the oil repellence of the surface (Li et al. 2013; Hubbe and Pruszynski 2020).

When an MFC coating is applied, it has been found that the coating process and base paper affect the coating uniformity (Aulin et al. 2010; Kumar 2017a; Padberg et al. 2017), and it has been suggested that with a thin coating layer or low coat weight, the MFC covers the pores of the substrate but that nanopores still remain in the coating. These nanopores merely retard the penetration of the oil and may not make the material grease-resistant. (Aulin et al. 2010; Lavoine et al. 2014).

Oil and grease resistance can be measured in various ways. The TAPPI T559 standard (Kit test) is used to determine the oil repellence of fluorochemical treated paper or paperboard, where the test solutions are used to determine the grease resistance. In the TAPPI T454 standard, turpentine is used to give an estimate of the rate of the penetration of oil and grease through greaseproof paper. In the ISO 16532-1 standard, palm kernel oil is used to determine the penetration time of grease through the material. In the ASTM F119 standard, the penetration of grease through flexible barrier materials is measured at standard conditions. The grease resistance obtained with different MFC types, coat weights and substrates with different test methods is presented in Table 5.2.

Table 5.2: Oil and grease resistance of MFC coatings (Paper III).

MFC type	Coat weight, [g/m^2]	Substrate	Grease resistance	Test method	Ref.
Native	3.2	Paper (machine-glazed)	1 g/m^2	SCAN P-37:77	1
Native	10	Paperboard	3.6 g/m^2 10 +	$Cobb_{30min}$ oil KIT test	2
Native	7	Paper	5.5	TAPPI T-559	3
Native	11	Paper	5.5	TAPPI T-559	3
Native	40	Paperboard	1 g/m^2 12	$Cobb_{30min}$ oil KIT test	2
Native CNF (refined)	8	Paperboard	0.5	TAPPI T-559	4
CNF (refined)	11	Paperboard	10	TAPPI T-559	5
Native CNF (ground)	12	Paperboard	9	TAPPI T-559	4
Native (enzymatic pretreatment)	7	Calendered paper	1	TAPPI T-559	6
Native (enzymatic pretreatment)	14	Calendered paper	5	TAPPI T-559	6
Native (enzymatic pretreatment)	14	Paperboard (C1S)	2.5	TAPPI T-559	7
CNF (native)	5	White kraft paper	7	TAPPI T-559	8
CNF	16	Paper	12	TAPPI T-559	9
Lignin containing CNF	16	Paper	12	TAPPI T-559	9
Native (+ plasticizer)	6.4	Pigment-coated paperboard	Max. ~3 days	ASTM F119	10
Native (+ plasticizer)	12.1	Pigment-coated paperboard	Max. ~ 7 days	ASTM F119	10
Carboxymethylated	1.1	Greaseproof paper	1800 s (castor oil)	TAPPI T-454	11
Carboxymethylated	1.8	Kraft	1800 s (castor oil)	TAPPI T-454	11
CNF	27-30 (films)	-	12	TAPPI T-559	12
CNF (thiol-norbornene modification)	27-30 (films)	-	12	TAPPI T-559	12

[1)] Boissard 2017 [2)] Guérin 2019 [3)] Padberg et al. 2017 [4)] Mousavi et al. 2018 [5)] Kumar et al. 2016 [6)] Lavoine et al. 2014 [7)] Lavoine et al. 2013 [8)] Tyagi et al. 2019 [9)] Tayeb et al. 2020 [10)] Koppolu et al. 2019 [11)] Aulin et al. 2010 [12)] Fein et al. 2020

6 Materials and methods

6.1 Materials

The 1 wt-% solutions were prepared with different proportions of hydrophobically modified ethyl(hydroxyethyl)cellulose (EHEC) (Bermocoll EHM200, AkzoNobel Functional Chemicals AB) and methyl nanocellulose (MeCellosic acid, MCA, Innotech Materials). The same proportions were used for hydrophobically modified EHEC-MFC (Celish KY100G, Daicel FineChem Ltd), hydrophobically modified EHEC-methyl nanocellulose and methyl nanocellulose-MFC solutions at 0.5 wt-% concentration in order to prepare cast films.

Methyl nanocellulose-based coating solutions were prepared with the addition of MFC and hydrophobically modified EHEC and also EHEC-MFC and MFC coating solutions were prepared. The coating was performed on uncoated, three-ply paperboard with a grammage of 190 g/m^2. The PPS_{10} roughness of the substrate was 6.2 µm (SCAN-P 76:95).

The EHEC-MFC (Celish KY100S, Daicel FineChem Ltd) solutions at concentrations of 1 and 3 wt-% and methyl nanocellulose solution at a concentration of 4 wt-% were prepared for foam coating. The foam coating was performed on paper substrates with a grammage of 100 g/m^2 and with different levels of smoothness and hydrophilicity or hydrophobicity. Calendering was performed to create a smoother surface using a nip pressure of 60 kN/m. The degree of hydrophobicity of the substrate was adjusted by varying the level of internal sizing agent (AKD).

6.2 Characterization of the solutions

6.2.1 Cloud point

The cloud points of the 1 wt-% EHEC-methyl nanocellulose solutions were detected visually as the point at which the solution turned cloudy, the change in turbidity being measured using a turbidimeter (Hach 2100AN IS Turbidimeter). The suspensions were sealed in glass tubes and were heated from 20 to 70 °C at a rate of 0.5 °C/min using a water bath.

6.2.2 Viscosity

The viscosity measurements were made with a Modular Compact Rheometer (MCR 302, Anton Paar, Austria) using a bob and cup mode. To determine the temperature-dependent behaviour, the viscosities of the 1 wt-% hydrophobically modified EHEC-methyl nanocellulose solutions and 0.5 wt-% hydrophobically modified EHEC-MFC and methyl nanocellulose-MFC solutions were measured at a shear rate of 50 s^{-1} while the solution

was heated from 20 to 70 °C at a rate of 0.5 °C/min. To avoid evaporation, a covering plate was used during the measurements. The gelation temperature was recorded as the point where the viscosity was at a minimum before it started to increase. The viscosities of the 1 and 3 wt-% EHEC-MFC and 4 wt-% methyl nanocellulose solutions were also measured at shear rates increasing from 0.1 to 1000 s^{-1}.

6.3 Preparation of cast films and coatings

The films were cast from solutions consisting of different ratios of microfibrillated cellulose and hydrophobically modified EHEC or methyl nanocellulose at a concentration of 0.5 wt-%. Air was removed from the MFC solution before the mixtures were prepared. The films were cast on petri dishes where the water was allowed to evaporate at 23 °C and 50 % relative humidity and at 50 °C. The targeted dry film grammage of the cast films was 30 g/m^2.

The methyl nanocellulose-based, hydrophobically modified EHEC-MFC and MFC coatings were prepared on a paperboard substrate with a DT Laboratory coater (DT Paper Science, Finland) with a soft-tip blade (BTG, Switzerland). Each coating layer was dried with an infra-red dryer. The viscosity of the coating solutions was measured with a Brookfield digital viscometer (Model DVII+, Brookfield Engineering Laboratories, Inc., USA) and was adjusted to approximately 2000 cP. The solids content, viscosity and pH of the coating solutions are presented in Table 6.1.

Table 6.1: Solids content, viscosity and pH of the coating solutions. Me indicates methyl nanocellulose. (Paper III).

Coating composition	Solids content, [%]	Viscosity, [cP]	pH
Me	10.5	1950	2.6
Me90:MFC10	5.7	2080	3.1
Me90:EHEC10	8.0	1860	2.9
EHEC90:MFC10	1.7	1960	5.3
MFC	2.3	1930	6.1

6.4 Foam analysis and foam coating

6.4.1 Foam density, viscosity and stability

Foams were generated with a foam generator (Rollmix BGR 13, Rollmac, Italy) and the properties of the generated foams were determined. The density was measured by weighing foam in a 100 ml measuring cylinder. A Brookfield digital viscometer (Model DVII+, Brookfield Engineering Laboratories, Inc., USA) was used to determine the viscosity at speeds of 10 and 50 rpm. The foam stability was defined as the degree to which the foam collapsed. Foam was collected in a 100 ml measuring cylinder, and the

collapse of the foam and the volume of liquid released from the foam were recorded after 60 minutes. The bubble size and the bubble size distribution of the foams were evaluated visually.

The gravimetric water retention meter (Åbo Akademi Gravimetric Water Retention method, ÅAGWR) was used to investigate the foam collapse and the release of water from the foam under pressure. For the measurement, 10 ml of foam was placed with a syringe into a sample cylinder, and a Whatman CHR 17 chromatographic paper was used as absorbing paper.

6.4.2 Foam coating

Paper substrates were coated with a desktop coater using a rod with wire having a diameter of 0.2 mm. The coating was dried at 105 °C after each coating layer had been applied. Three coating layers were applied on the substrate.

6.5 Evaluation of film formation and barrier properties

6.5.1 Grammage, thickness and air permeance

The grammage, thickness and air permeance of the uncoated and coated materials were measured according to the SCAN P-6:75, SCAN P-7:75 and SCAN P-85:02 standards, respectively. The coating thickness and coat weight were calculated by subtracting the thickness and grammage of the uncoated material from the thickness and grammage of the coated material, respectively. All the samples were conditioned at 23 °C and 50 % relative humidity prior to the measurements.

6.5.2 Surface imaging

Roughness of the cast films was determined with atomic force microscope (AFM, Bruker Multimode 8 AFM, Bruker, USA). Measurements from the cast films were obtained using the tapping mode and PeakForce QNM (quantitative nanomechanical mapping) mode and probe with a spring constant of 81 N/m and a tip radius of ca. 70 nm. For The EHEC-MFC sample, two PeakForce QNM readings were analyzed and three readings for the other samples. NanoScopeAnalysis 1.5 software was used to analyze the QNM data. Roughness values were calculated as root mean square averages (R_q) of height deviations (z_i) for 5 x 5 µm areas:

$$R_q = \sqrt{\frac{\sum z_i^2}{N}} \tag{6.1}$$

An FE-SEM image of the surface was obtained using a FEI Nova NanoSEM 450 field emission scanning electron microscope (FE-SEM) with a Schottky type emitter. A Hitachi IM4000 broad ion beam cross section cutter was used for preparing the cross-section of the sample. The sample was glued on a copy paper with a solvent-free glue to obtain a rigid sample for cutting. The working distance was 5.0 mm and the acceleration voltage 5.0 kV (Paper II).

A scanning electron microscope Hitachi SU3500 with a secondary electron (SE) detector was used to capture images of the uncoated and coated samples which were sputter-coated with gold prior to measurement. The acceleration voltage and working distance were respectively 5.0 kV and approximately 9 mm (Paper III) and 10.0 kV and 5 mm (Paper IV).

6.5.3 Wetting of the films and determination of surface energy

The wetting of cast films and both uncoated and coated surfaces was evaluated with contact angle determinations (Attension Theta Optical Tensiometer, Biolin Scientific AB, Sweden) using rapeseed oil with a drop volume of 5 µl. The wetting of the coated surfaces was also evaluated using deionised water and a drop volume of 3 µl.

The surface energy of the cast films was determined using deionized water, ethylene glycol (VWR S.A.S. International) and diiodomethane (Alfa-Aesar GmbH & Co KG). Drop volumes were 3 µl for deionized water and ethylene glycol and 1 µl for diiodomethane. The contact angles were determined one second after placing the drop on the surface. The calculation of surface energy (γ) of the solid (s) was based on the contact angles (θ) of one non-polar and two polar liquids (li) and an equation which sums the Lifschitz-van der Waals (LW), electron acceptor (+) and donor (-) components (Hejda et al. 2010):

$$(1 + cos\theta_i)\gamma_{li} = 2\left(\sqrt{\gamma_{li}^{LW}\gamma_s^{LW}} + \sqrt{\gamma_{li}^{+}\gamma_s^{-}} + \sqrt{\gamma_{li}^{-}\gamma_s^{+}}\right) \quad (6.2)$$

6.5.4 Barrier properties

The oxygen transmission rate (OTR) of the cast films was measured using a Mocon Ox-Tran Model 2/22 (Mocon, USA) with the test conditions of 23 °C and 50 % RH. The reported OTR values are average values of three independent measurements.

The oil and grease resistance (OGR) of the coated paperboards was measured using the ISO 16532-1 standard and the OGR of the cast films was measured with a modified method, without any applied weight on the oil drop. The oil and grease resistance of the coatings was also measured using rapeseed oil with or without an applied weight on the oil drop at 23 °C and 50 % RH.

7 Results and discussion

7.1 Methyl nanocellulose, MFC and hydrophobically modified EHEC in aqueous solution

The interaction and clouding behaviour of EHEC and methyl nanocellulose at 1.0 wt-% concentration were studied with the cloud point determinations (Paper I). To investigate the effect of temperature on the interaction between hydrophobically modified EHEC-methyl nanocellulose at 1 wt-% concentration (Paper I), and between hydrophobically modified EHEC-MFC and methyl nanocellulose-MFC at 0.5 wt-% concentration (Paper II), the viscosities of the different compositions were measured while the solution was heated. The cloud point and viscosity measurements were also made on pure hydrophobically modified EHEC and methyl nanocellulose solutions at different concentrations (Paper I).

7.1.1 Cloud point

The turbidity and cloud point values are presented in Figure 7.1. In the case of the EHEC-methyl nanocellulose compositions, the initial turbidity of the solutions decreased with increasing proportion of methyl nanocellulose and was the lowest for the 100 % methyl nanocellulose solution (Figure 7.1(a)). The EHEC-methyl nanocellulose solutions showed an increase in turbidity when they were heated to 25 °C. When the heating was continued, the turbidity started to decrease, but started to increase again when the temperature reached 40 °C. When the methyl nanocellulose-containing solutions reached the cloud point temperature, the turbidity increased rapidly and the increase was more pronounced with increasing methyl nanocellulose content.

The pure hydrophobically modified EHEC solution showed a relatively low cloud point temperature, at 25-30 °C (Figure 7.1(b)). The cloud point temperature of the hydrophobically modified EHEC depends on the length of the hydrophobic groups and can be lower than room temperature (Karlson et al. 2000). The highest cloud point was observed for the EHEC-methyl nanocellulose solution with a ratio of 25:75.

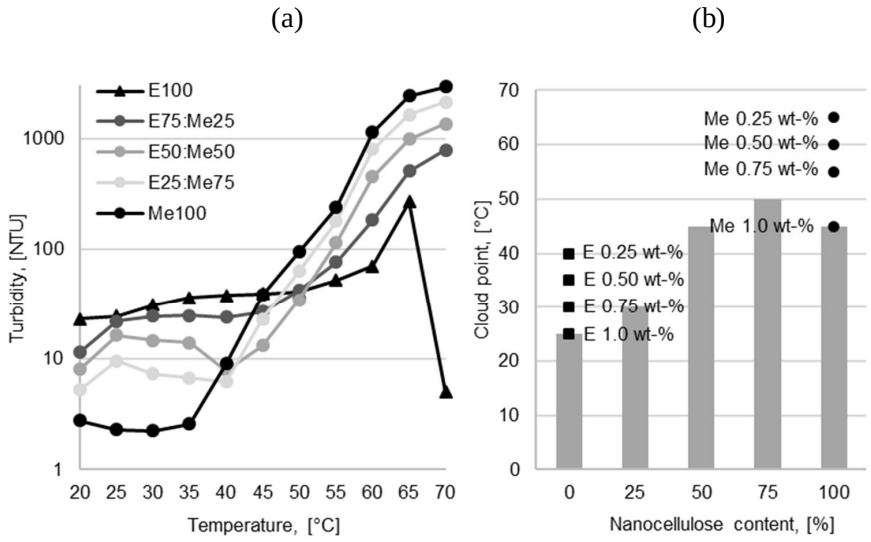

Figure 7.1: The (a) turbidity and (b) cloud point temperatures of the EHEC-methyl nanocellulose solutions at 1 wt-% concentration. Squares and dots in Figure 7.1(b) refer to the cloud points of respectively hydrophobically modified EHEC (E) and pure methyl nanocellulose (Me) at different concentrations.

The turbidity of the EHEC-methyl nanocellulose solutions is shown in Figure 7.2. Before they were heated, all the solutions were clear. The pure hydrophobically modified EHEC and the EHEC-methyl nanocellulose solution in a ratio of 75:25 were cloudy at 35 °C, with cloud points of 25 °C and 30 °C, respectively. Macromolecular phase separation in hydrophobically modified EHEC-methyl nanocellulose solutions in the form of small flocs or particles was observed at 45 °C in the solutions with ratios of 50:50 and 25:75 and at 55 °C in the solution with a ratio of 75:25. The methyl nanocellulose-containing solutions showed a rapid increase in turbidity when the cloud point temperature was reached.

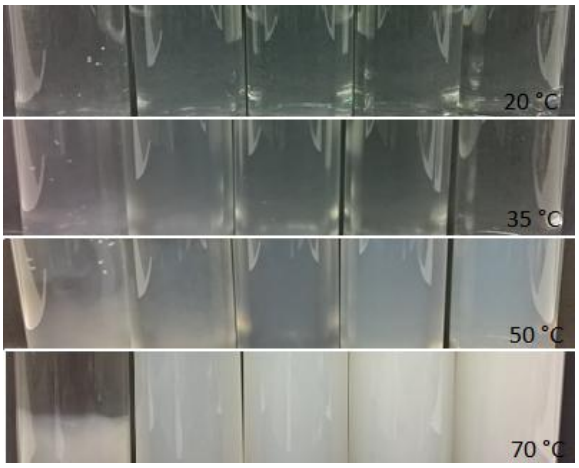

Figure 7.2: The turbidity of EHEC-methyl nanocellulose solutions in a ratio of 0:100, 75:25, 50:50, 25:75 and 0:100 at different temperatures.

In general, the presence of methyl nanocellulose in the solutions raised the cloud point, whereas an increase in solids content in the pure hydrophobically modified EHEC and methyl nanocellulose solutions lowered the cloud point. Changes in phase behaviour and cloud point temperatures have been observed in studies of the effect of surfactant binding to EHEC. It is also known that the cloud point is affected by the salt concentration. A high concentration of salt leads to a decrease in the cloud point since the solubility of the EHEC is decreased. The hydrophobically modified EHEC solution contained salt, and the lower amount of hydrophobically modified EHEC in the compositions may thus also have affected the cloud point.

7.1.2 **Viscosity**

Figure 7.3 shows that the viscosity of the pure hydrophobically modified EHEC decreased with increasing temperature whereas that of the methyl nanocellulose first decreased and then started to increase at the gelation temperature. Both hydrophobically modified EHEC and methylcellulose showed thermoresponsive behaviour at elevated temperatures presumably due to hydrophobic association and phase separation (Thuresson and Lindman 1997, Arvidson et al. 2013), but the association between hydrophobically modified EHEC molecules is weak and breaks easily under shear. The gelation of the methyl nanocellulose is affected by the concentration; the gelation temperature decreased and the gelation was more pronounced with increasing concentration.

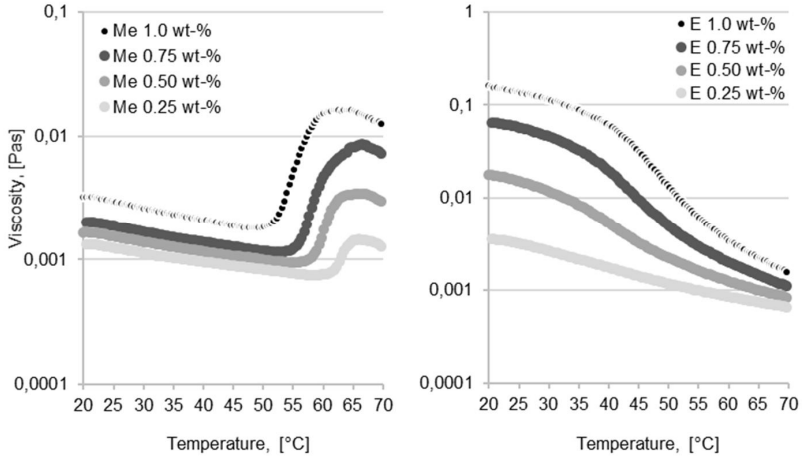

Figure 7.3: The effect of concentration on the viscosity of pure methyl nanocellulose (Me) and of hydrophobically modified EHEC (E) solutions at different temperatures.

The interaction between the components was expected to affect the viscosity and gel behaviour. Figure 7.4(a) shows that the viscosity of the EHEC-methyl nanocellulose mixtures was lower at a given concentration than the pure hydrophobically modified EHEC solutions, which is due to the lower viscosity of the methyl nanocellulose. The initial viscosity of the EHEC-methyl nanocellulose solution in a ratio of 25:75 was higher than that of the 0.25 wt-% hydrophobically modified EHEC solution and its gelation temperature was two degrees lower than that of the methyl nanocellulose solution at 0.75 wt-% concentration.

The viscosity of the 0.5 wt-% MFC suspension decreased with increasing temperature (Figure 7.4(b)). The EHEC-MFC solutions showed a decreasing viscosity with increasing temperature especially with low additions of MFC. Due to the higher viscosity of the MFC, the initial viscosity of the EHEC-MFC solutions was expected to be higher than the viscosity of hydrophobically modified EHEC, but at ratios of 25:75 and especially when the ratio was 50:50 the viscosity was lower, suggesting that there was an interaction between the components. Compared to the pure MFC and other EHEC-MFC solutions, the viscosity of the EHEC-MFC in a ratio of 25:75 was stable and started to decrease when the temperature reached 35 °C.

With increasing addition of MFC in the methyl nanocellulose-MFC solutions, the initial viscosity increased (Figure 7.4(c)). All the methyl nanocellulose-containing solutions showed gelation at elevated temperature. The viscosity of the methyl nanocellulose-MFC solutions was however stable before gelation. The viscosity of the methyl nanocellulose-MFC solution in a ratio of 25:75 increased slightly when the heating started but started to decrease when the temperature reached 30 °C. The changes in gelation temperature may indicate an interaction between methyl nanocellulose and MFC at ratios of 75:25 and

50:50, since they showed a gelation temperature lower than that of pure methyl nanocellulose solution, although the gelation temperature should increase with decreasing concentration of methyl nanocellulose.

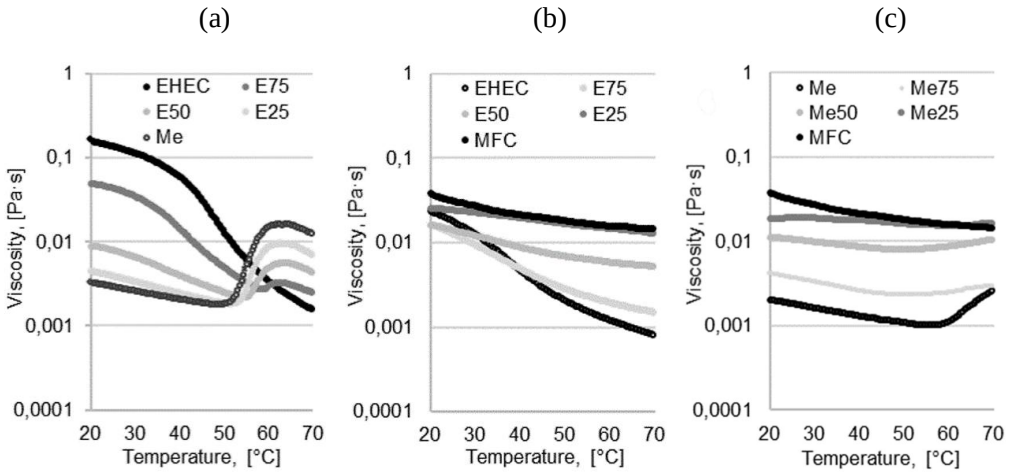

Figure 7.4: Viscosities of (a) EHEC-methyl nanocellulose at 1 wt-% concentration, (b) EHEC-MFC at 0.5 wt-% concentration and (c) methyl nanocellulose-MFC at 0.5 wt-% concentration as functions of temperature. Both EHEC and E refer to hydrophobically modified EHEC and Me to methyl nanocellulose.

Figure 7.5 shows the viscosities of the hydrophobically modified EHEC-MFC and methyl nanocellulose solutions as a function of shear rate (Paper IV). The mixtures of EHEC and a coarser native microfibrillated cellulose in a ratio of 25:75 were shear thinning. In the 1 wt-% solution, an increase in viscosity was observed at a shear rate between 1 and 5 s^{-1} which is characteristic of MFC solutions. The viscosity peak disappeared with increasing solid content, as has been observed by others for MFC suspensions at higher solids content (Iotti et al. 2011). When the solids content of the MFC suspension was increased, the viscosity increased significantly with a more rigid structure which also affects the formation of flocs and subsequently the properties of the coating. The addition of CMC has been found to reduce the formation of flocs (Kumar et al. 2017b). The viscosity of the methyl nanocellulose solution showed a Newtonian behaviour independent of shear rate, although small changes were seen at very low shear rates.

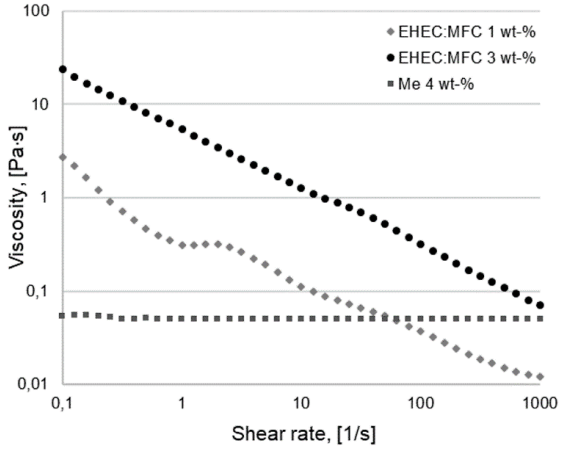

Figure 7.5: The viscosity of the EHEC-MFC solutions at a ratio of 25:75 at 1 and 3 wt-% concentrations and of methyl nanocellulose at 4 wt-% concentration as a function of shear rate.

7.1.3 **Foam formation and foam stability**

Amphiphilic polymers such as hydrophobically modified EHEC can be used to stabilize foams, and the ability of the system to foam and stabilize air bubbles was investigated. The aim was to prepare a stable foam suitable for foam coating and to use air as carrier phase to create a dense film on the substrate (Paper IV).

EHEC-MFC and methyl nanocellulose foams were generated with a foam generator, and the main properties of the foams are presented in Table 7.1. Foams with a density above 20 g/100 ml are referred to as wet foams (Kinnunen-Raudaskoski et al. 2014), and all the foams selected for foam coating in this study were thus wet foams. The EHEC-MFC foam generated from 3 wt-% solution had the highest viscosity and the viscosity of the EHEC-MFC foams was dependent on the concentration. An increase in viscosity and the stability of the foam has been explained as being due to the hydrogen bonding between the fibrils, and weak bonding has been associated to a less stable foam (Li et al. 2019). The bubble size and the bubble size distribution were evaluated visually and were found to be greatest in the methyl nanocellulose foam and smallest in the EHEC-MFC foams.

The collapse of foam and the release of water under light pressure was evaluated by gravimetric water retention (ÅAGWR) measurements. The water-holding capacity of the MFC is high (Kumar et al. 2017b) and was observed as a decreasing amount of liquid released from the EHEC-MFC foam when the solids content was increased. The water release from the methyl nanocellulose foam was significantly higher than that released from the EHEC-MFC foam with a higher solids content. In addition, the EHEC-MFC foams, especially that generated from the 3 wt-% solution, remained almost unchanged during the ÅAGWR measurement, whereas the methyl nanocellulose foam showed a significantly greater tendency to collapse. These results confirm that the methyl

nanocellulose foam was less stable, since the water release from the structure was higher and it broke more easily under the applied pressure. The solids content of methyl nanocellulose foam was however the same as that of the solution before foaming, indicating that there was a uniform distribution of the material in the foam.

Table 7.1: Properties of the EHEC-MFC foams generated from the 1 and 3 wt-% solutions and methyl nanocellulose foam generated from 4 wt-% solution. S.c. refers to solids content.

	pH, Solution	s.c., [%]	Density, [g/100 ml]	ÅAGWR, [g/m^2]	Viscosity, [10 rpm, cP]	Viscosity, [50 rpm, cP]
			EHEC25:MFC75			
1 wt-%	6.0	0.94	25.4	1267	1960	680
3 wt-%	6.7	2.46	45.0	289	9280	3488
			Methyl nanocellulose			
4 wt-%	2.9	4.01	39.1	3884	3360	1500

The stability of the foams was recorded by determining the amount of liquid released and collapsed foam during a period of 60 minutes. In general, the EHEC-MFC foams (Figures 7.6(a) and 7.6(b)) were more stable than the methyl nanocellulose foam (Figure 7.6(c)). Liquid was released from the EHEC-MFC foam generated from the 1 wt-% solution during this time, but at higher solids content no foam collapse was observed. The water-holding capacity and stability of methyl nanocellulose foam were significantly lower than that of the EHEC-MFC foams and the amount of liquid released during this time was high compared to the density of the foam.

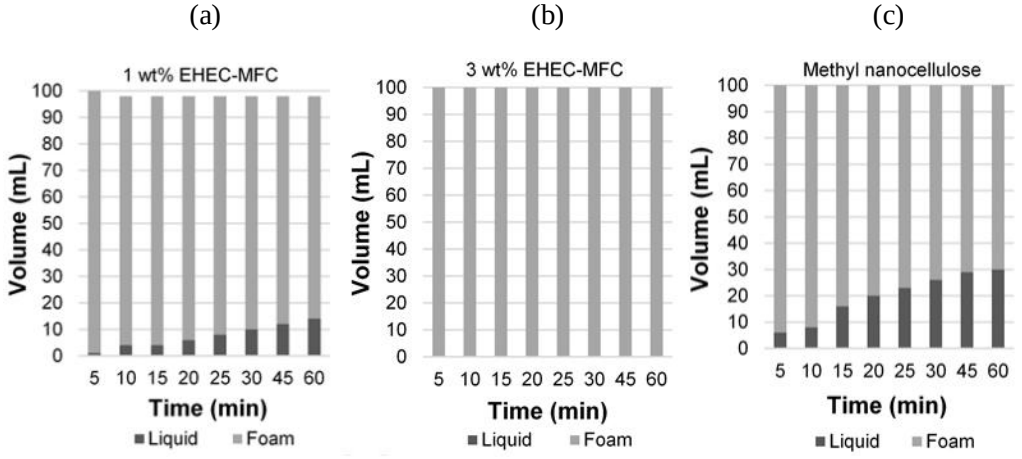

Figure 7.6: Stability of the (a) 1 wt- %, (b) 3 wt-% hydrophobically modified EHEC-MFC foams in a ratio of 25:75 and (c) 4 wt-% methyl nanocellulose foam. A larger amount of liquid released and foam collapse indicate a less stable foam.

The viscosity and the gravimetric water retention measurements showed that the methyl nanocellulose foam was less stable than the EHEC-MFC foams. Larger bubbles and a broader size distribution were observed, and these decrease the stability of the foam (Kinnunen-Raudaskoski et al. 2014). The increased stability and the smaller amount of liquid released from the EHEC-MFC foam in the gravimetric water retention measurements indicate that there is a larger amount of MFC between the bubbles (Xiang et al. 2019).

7.2 Cast films and coatings

7.2.1 Cast films

Cast films were prepared from 0.5 wt-% solutions of hydrophobically modified EHEC and MFC, hydrophobically modified EHEC and methyl nanocellulose and methyl nanocellulose and MFC (Paper II). The differences in transparency between the films were significant. The pure methyl nanocellulose and hydrophobically modified EHEC films were transparent, but the films were more opaque when the proportion of MFC was increased (Figures 7.7(a), 7.7(b) and 7.7(d)) and the transparency of the films containing both EHEC and methyl nanocellulose decreased with increasing proportion of methyl nanocellulose in the film (Figure 7.7(c)). The transparency of the EHEC-MFC films was clearly affected by the drying temperature as the EHEC-MFC films were more transparent when they were dried at a higher temperature (Figure 7.7(b)). Air bubbles were observed in the EHEC-MFC and methyl nanocellulose-MFC films when they were dried at elevated temperature.

Air bubbles were formed in the EHEC-MFC and methyl nanocellulose-MFC films especially at a ratio of 25:75 and when the drying temperature was 50 °C. Some bubbles were also formed in the MFC films at this temperature. The bubbles in the MFC films could be partially explained by the roughness of the petri dish or changes in surface energy, since no air bubbles were formed when the surface of the petri dish was wetted before casting. The stability of the EHEC-MFC and methyl nanocellulose-MFC solutions or that the film surface dries faster at the higher temperature may have promoted the trapping of air bubbles in the film. The air bubbles occurred at the ratios at which the viscosity remained most stable when the EHEC-MFC and methyl nanocellulose-MFC solutions were heated.

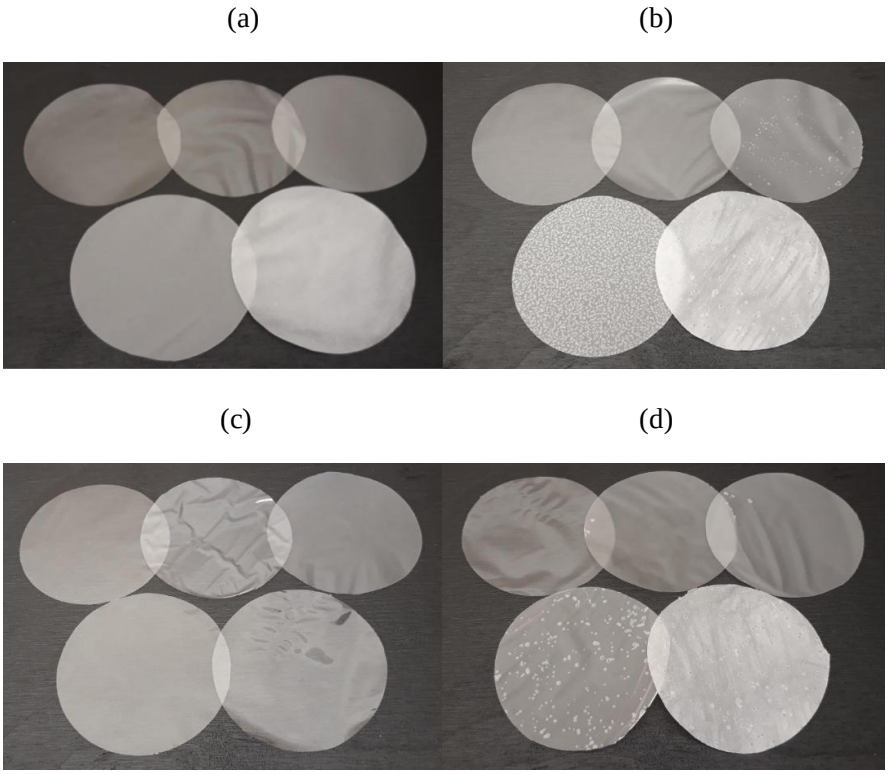

Figure 7.7: Cast EHEC-MFC films dried at (a) 23 °C and (b) 50 °C. (c) EHEC-methyl nanocellulose and (d) methyl nanocellulose-MFC films dried at 50 °C. The films were prepared in ratios of 100:0, 75:25, 50:50 (upper row), 25:75 and 0:100 (lower row).

Air bubbles were not formed in the EHEC-methyl nanocellulose films. The transparency of the films consisting of both hydrophobically modified EHEC and methyl nanocellulose was lower than that of the pure hydrophobically modified EHEC and methyl nanocellulose films, although all the EHEC-methyl nanocellulose solutions were cloudy at 50 °C. This suggests that the particle size of the EHEC-methyl nanocellulose solution increased at a higher temperature, since larger particles scatter more light (Hubbe et al. 2017). On the other hand, a more opaque film indicates an agglomeration, attributed to the incompatibility of the components (Hubbe et al. 2017), but the changes in cloud point and viscosity suggest an interaction between the components.

The quantity of the air bubbles was significantly higher in the EHEC-MFC film (Figure 7.8(a)) and the air bubbles were more coalesced and smaller than in the methyl nanocellulose-MFC film (Figure 7.8(b)). The bubbles were white in the EHEC-MFC and methyl nanocellulose-MFC films, suggesting that the fibrils are on the surface of the bubbles and thus scatter light more. Some air bubbles were formed in the MFC films, but they were more transparent than in the other films (Figure 7.8(c)).

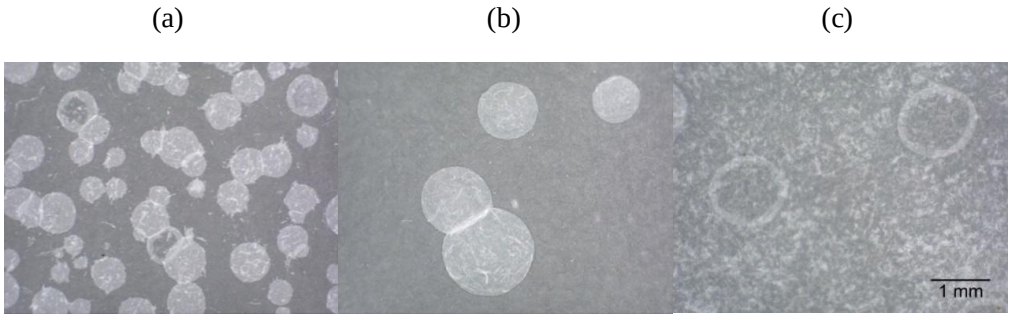

Figure 7.8: The bubble formation in (a) EHEC-MFC, (b) methyl nanocellulose-MFC, (c) MFC films dried at 50 °C. All the compositions were in a ratio of 25:75.

Although the air bubbles were formed in the EHEC-MFC film, the film was continuous as shown in Figure 7.9. Since no bubbles were observed in the films dried at 23 °C, the presence of the air bubbles appeared to be due to the faster drying of the surface at the higher temperature which formed a skin on the surface together with a rapid increase in viscosity, trapping the air bubbles into the surface in the film. This suggests that there is a certain EHEC-MFC composition that enhances bubble formation and stabilizes the bubbles.

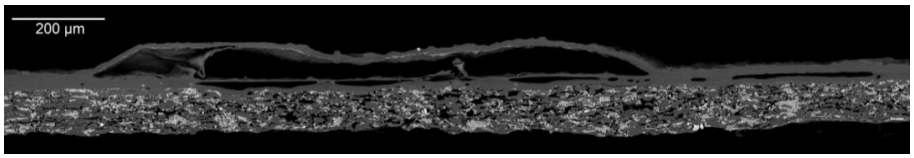

Figure 7.9: SEM-image of an air bubble formed in the EHEC-MFC film. A copy paper was used as a carrier medium for the sample.

7.2.2 Coating with non-foamed solutions

Figure 7.10 shows the methyl nanocellulose-based coatings with the addition of MFC or hydrophobically modified EHEC, hydrophobically modified EHEC-MFC and MFC coatings applied to a paperboard substrate (Paper III). The highest coat weight was achieved with methyl nanocellulose and methyl nanocellulose-MFC coatings with coat weights of 10 g/m^2 and 9 g/m^2, respectively, but blistering occurred in both coatings. The coating coverage was similar for the methyl nanocellulose and methyl nanocellulose-MFC coating, although methyl nanocellulose-MFC coating solution had lower solid content than that of the methyl nanocellulose. The coating coverage of the methyl nanocellulose-EHEC coating seemed to be relatively high, but defects were observed in the coating. The EHEC-MFC and pure MFC coatings gave the lowest coat weights and poorest coating coverage.

It is possible that air bubbles were formed in the coating solution during coating process and that this led to blistering. The bubbles may also have affected the transfer of the coating solution onto the substrate, leading to defects in the coating. Although pinholes occurred in the coatings, another coating layer was in most cases observed under the pinhole, and the defect did not go through all the coating layers. The methyl nanocellulose-EHEC coating also had cracks related to the presence of the hydrophobically modified EHEC in the coating.

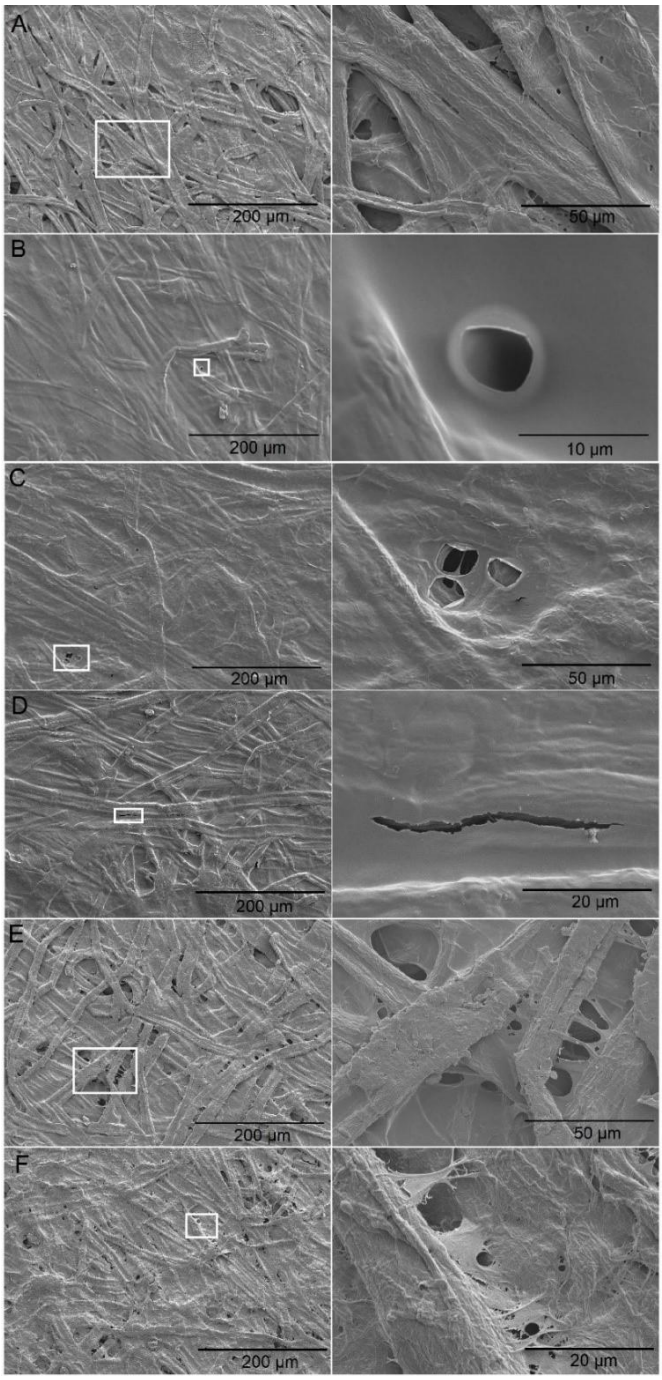

Figure 7.10: SEM micrographs of (a) uncoated substrate and of (b) methyl nanocellulose, (c) methyl nanocellulose-MFC, (d) methyl nanocellulose-EHEC, (e) EHEC-MFC and (f) MFC coatings after five coating layers.

7.2.3 Foam coating

To compare the coat weights and coating coverage achieved with foam and non-foamed solutions, 1 wt-% solutions consisting of hydrophobically modified EHEC and methyl nanocellulose were prepared (Paper IV). An uncoated internally sized paperboard was used as a substrate which was coated three times, and the air permeance and coat weight were determined of the coated materials (Figure 7.11).

The highest coat weights were obtained with the pure hydrophobically modified EHEC and methyl nanocellulose with both non-foamed and foamed solutions. Both non-foamed and foam coatings reduced the air permeance compared to that of the uncoated substrate which had an air permeance of 580 ml/min. The same air permeance or lower was achieved with foam coating as with non-foamed solution, except when the EHEC-methyl nanocellulose ratio in the foam was 25:75. The greatest reduction in air permeance and the lowest coat weights were obtained with coatings consisting of hydrophobically modified EHEC and methyl nanocellulose in the ratios of 75:25 and 50:50. With the EHEC-methyl nanocellulose in a ratio of 25:75, the viscosity and cloud point measurements suggested an interaction between the components, which may have reduced the stability of the foam or increased the particle size and led to an uneven coating coverage.

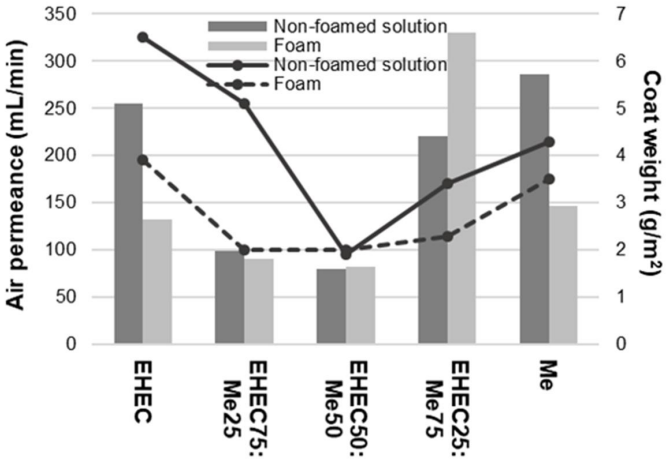

Figure 7.11: Coat weight and air permeance after coating with non-foamed solution and foam coatings on a paperboard substrate. Coatings consisted of hydrophobically modified EHEC and methyl nanocellulose (Me). The air permeance of the uncoated material was 580 ml/min. The solid line shows the coat weight obtained with non-foamed solutions and the dashed line that obtained with a foam coating. Columns show the air permeance of the coated substrates.

SEM-images showed that the collapsed methyl nanocellulose and EHEC-methyl nanocellulose foams (Figures 7.12(a) and 7.12(c)) closed the surface of the substrates more compared to the coatings with the non-foamed solutions (Figures 7.12(b) and 7.12(d)). After the foam coating, the surface seemed to be more even and closed, suggesting that the foam collapses uniformly and has a better film-formation ability compared to that of the non-foamed solution. The EHEC-methyl nanocellulose foam (Figure 7.12(d)) gave a smoother surface, indicating that the foam was more stable and penetrated less into the substrate.

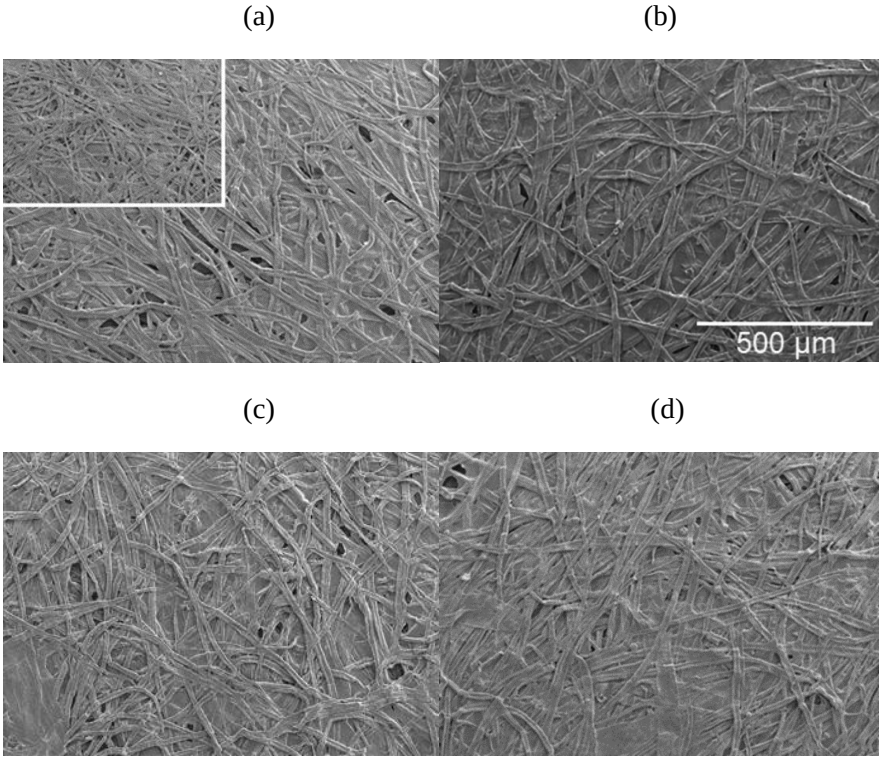

Figure 7.12: Non-foamed (a) methyl nanocellulose and (c) EHEC-methyl nanocellulose coatings, and (b) methyl nanocellulose and (d) EHEC-methyl nanocellulose foam coatings. The EHEC-methyl nanocellulose coating composition was in a ratio of 50:50. The image of the uncoated substrate is shown as an inset in image A.

In EHEC-MFC cast films in a ratio of 25:75, air bubbles were formed unintentionally in the films, which indicated that a certain EHEC-MFC composition enhances the bubble formation and stabilization of bubbles and could thus also be able to form a stable foam suitable for foam coating. The EHEC-MFC and methyl nanocellulose solutions were selected for foam coating on papers with different hydrophobicities, hydrophilicities and smoothness in order to evaluate the role of the substrate in foam coating (Paper IV).

SEM images of the EHEC-MFC and methyl nanocellulose foam coatings on calendered hydrophilic and hydrophobic substrates are presented in Figure 7.13. The coating coverage seems to be higher on the hydrophilic substrate with the EHEC-MFC coating, but the coating seems uneven on hydrophobic substrate and the surface is not entirely covered. In the case of the methyl nanocellulose, the surface appears to be more even on both substrates, but it is more uniform on the hydrophilic substrate. On the other hand, the solids content was higher in the methyl nanocellulose foam and this shall give a more uniform distribution of the material in the foam and lead to a greater coating coverage. However, wrinkling occurred in the hydrophilic substrate after coating, probably due to the lower stability and water retention of the methyl nanocellulose foam which facilitate the wetting of the substrate. In addition, the hydrophilic substrate may promote collapse of the foam and thus greater wetting in contrast to the hydrophobic substrate where foam may collapse more due to the applied pressure in the doctoring. This may have increased the penetration of the coating into the hydrophobic substrate, but collapse may be more controlled and favour the formation of a more uniform coating under applied pressure.

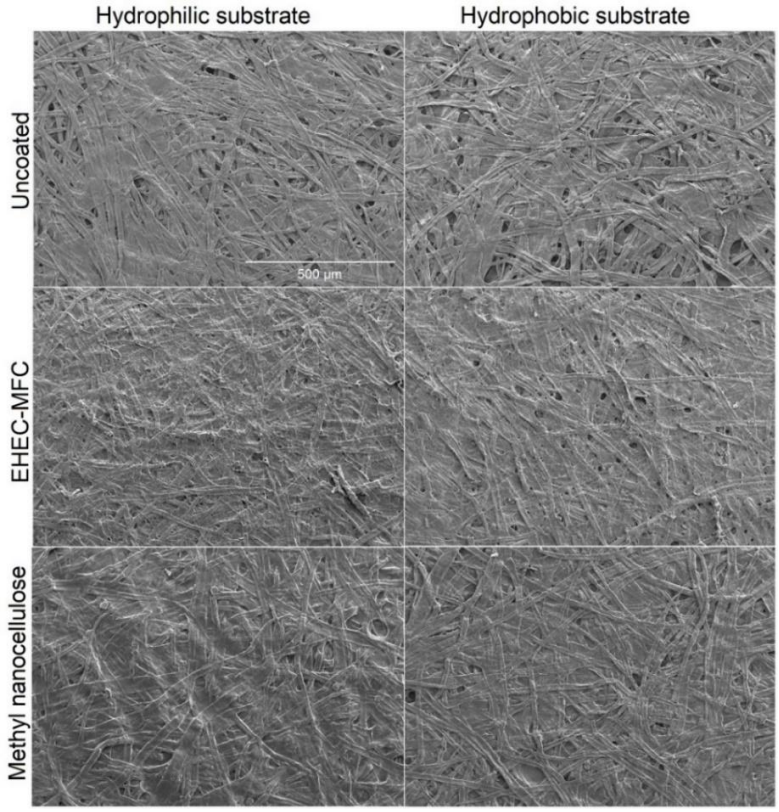

Figure 7.13: Uncoated and calendered hydrophilic and hydrophobic substrates and EHEC-MFC and methyl nanocellulose coatings on these substrates. The coated samples had three coating layers.

Higher hydrophilicity may increase the transfer of coating solution into the substrate. This may partially explain the higher coat weight of the EHEC-MFC coating on the hydrophilic substrate, and it may also explain the lower coat weight of non-foamed MFC and methyl nanocellulose-MFC solutions after one coating layer when the coating was applied to the hydrophobic paperboard. The viscosity of the coating solution may also affect the coat weight.

With both non-foamed solutions and foam, defects such as blistering and cracks developed, and were related more to the process than to the base paper or paperboard. In the non-foamed solution, air bubbles formed unintentionally and they may remain in the coating and result in pinholes due to excessive drying. Blistering was also observed with the foam coating, but the coating layer under the bubble remained uniform indicating that a multi-layer structure can be formed creating a grease barrier. However, foam coating requires optimization of the foam stability, since too low stability may result in an uneven coating due to large bubbles. The foam should rupture on the substrate under the applied pressure to create a dense film without defects.

7.3 Film and coating properties

7.3.1 Surface energy and wetting of the films

The surface energy was determined for the hydrophobically modified EHEC-MFC, methyl nanocellulose-MFC and hydrophobically modified EHEC-methyl nanocellulose cast films in a ratio of 25:75 and for the pure methyl nanocellulose film (Paper II). The surface energy was highest in the pure methyl nanocellulose film, 39 mN/m, although the hydrophobically modified EHEC-containing films also had a high surface energy. The methyl nanocellulose-MFC film had a significantly lower surface energy when the surface energy was calculated using the Equation 6.2.

The wetting and absorption properties of the surfaces were evaluated from contact angle determinations using rapeseed oil or water. The change in the oil or water drop within 10 seconds was measured. The spreading of the oil on cast films is shown in Figure 7.14 (Paper II). After the drop was placed on to the surface, the contact angle decreased by nearly 20° on all the surfaces within one second. On the hydrophobically modified EHEC-containing films, the oil spread laterally almost completely within 10 seconds. The roughness of the EHEC-MFC film dried at an elevated temperature (Figure 7.14(a)) was higher than that of the EHEC-methyl nanocellulose (Figure 7.14(c)) or EHEC-MFC film dried at a lower temperature (Figure 7.14(d)), and this can explain the minor differences between the samples. In the case of the methyl nanocellulose-MFC film, only a minor change in the contact angle was observed between one and ten seconds (Figure 7.14(b)). The surface energy was not found to correlate with the oil behaviour on the hydrophobically modified EHEC-containing films, although the methyl nanocellulose had the lowest surface energy and the highest contact angle with oil. The difference in spreading of oil on the EHEC-MFC and methyl nanocellulose-MFC films suggests that

the MFC in the films was covered by EHEC or methyl nanocellulose and also that the hydrophobically modified EHEC facilitates the spreading of oil on the surface.

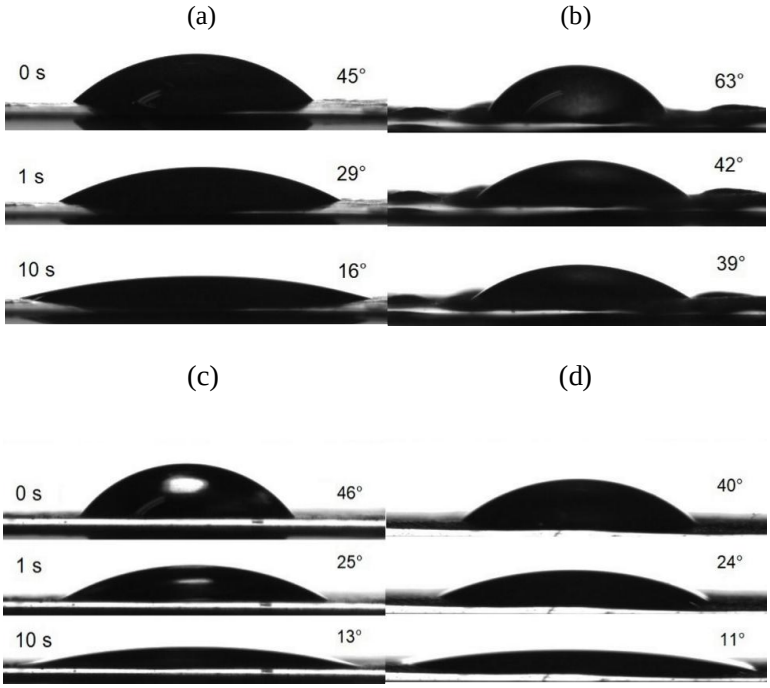

Figure 7.14: The spreading of oil on the (a) EHEC-MFC, (b) methyl nanocellulose-MFC and (c) EHEC-methyl nanocellulose films dried at 50 °C and on (d) EHEC-MFC film dried at 23 °C.

To evaluate the wetting of the coated samples, the contact angles of water and oil were determined on uncoated and five times coated surfaces (Figure 7.15) (Paper III). The contact angle for oil was similar on the uncoated substrate and the MFC and EHEC-MFC coatings, as shown in Figure 7.15(a), but the contact angle of water was significantly higher on the EHEC-MFC coating which suggests that the hydrophilic MFC is covered by the hydrophobically modified EHEC layer. The hydrophobicity may also explain the lower contact angle of oil due to the changes in polarity. The methyl nanocellulose-containing coatings had the highest oil contact angles. The differences in the contact angles of oil and water between methyl nanocellulose-containing coatings were not significant.

The spreading and absorption of the oil drop is presented in Figure 7.15(b). On the uncoated sample, the oil was absorbed, since the base of the oil drop did not change, but the volume of the oil drop decreased. Similar behaviour was observed on the methyl nanocellulose-containing coatings, as methylcellulose provides a barrier and prevents oil absorption (Nasatto et al. 2015), and thus the changes were not as great as on the uncoated

sample. In addition, the surface energy of the methyl nanocellulose film was higher than that of the methyl nanocellulose-MFC film, but the oil drop behaviour was similar on the two coated surfaces. On the surfaces coated with EHEC-MFC solution and MFC, oil spread on the surface. The wetting on the coatings was similar to that on the cast films, although the amount of the methyl nanocellulose in the compositions was higher than the ratio in the cast films.

(a) (b)

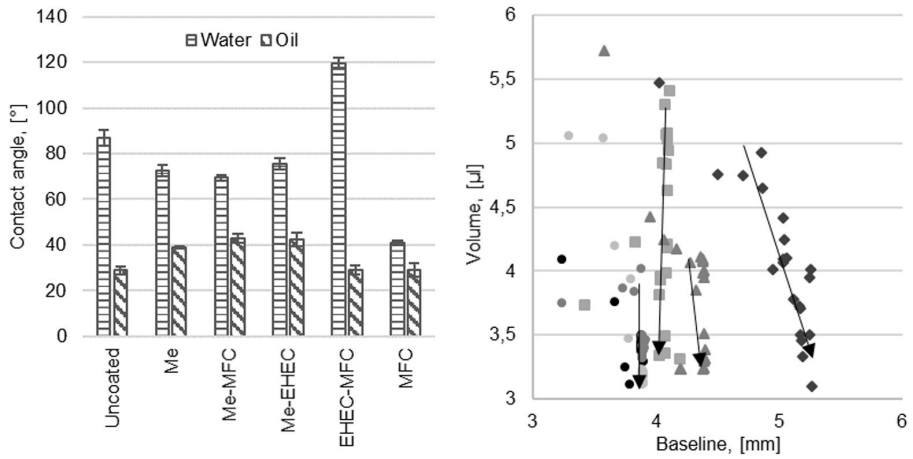

Figure 7.15: (a) Contact angles of oil and water on the uncoated and coated materials. (b) The change in oil drop volume on uncoated and coated surfaces during 10 seconds after placing the drop on the surface. Squares indicate uncoated surface, diamonds EHEC-MFC, triangles MFC and black, grey and light grey dots methyl nanocellulose, methyl nanocellulose-MFC and methyl nanocellulose-EHEC coatings, respectively. The arrows show the direction of change.

Contact angles were determined on uncoated and foam coated samples using rapeseed oil and water (Paper IV). On the uncoated surfaces, the contact angle of oil was lowest on the hydrophilic and calendered surface (Figure 7.16(a)). The water drop was rapidly absorbed by the hydrophilic substrates and was not measurable on the uncalendered material and calendering had only a minor effect (Figure 7.16(b)). The contact angle of water on the uncoated hydrophobic substrate was however almost 120°.

In general, the coat weights achieved with foam coating after three coating layers were low. Hydrophobically modified EHEC-MFC coating increased the oil absorption and spreading on all the substrates (Figure 7.16(c)) the oil being absorbed within five seconds. Methyl nanocellulose coatings on the hydrophilic substrate increased the contact angle of oil (Figure 7.16(e)), and similar behaviour was observed with cast films and coating with non-foamed solutions when methyl nanocellulose-MFC composition and methyl nanocellulose were used. SEM-images showed that the methyl nanocellulose coating on

the hydrophobic surface may have penetrated into the substrate, and this may explain the lower contact angles of oil since there is no significant difference in the coat weight. The spreading or absorption of oil were less on the calendered hydrophobic substrate.

Both the EHEC-MFC and methyl nanocellulose coatings significantly increased the contact angle of water compared with hydrophilic uncoated surface (Figures 7.16(d) and 7.16(f)). The increase was greater on the EHEC-MFC coating. The contact angle of water decreased more within 5 seconds on the hydrophilic and calendered substrate, where the SEM images (Figure 7.13) indicated that the amount of MFC on the surface was higher. The contact angles of water were lower on the hydrophobic surface after both EHEC-MFC and methyl nanocellulose coatings. In the case of methyl nanocellulose, the higher contact angle of water and the different behaviour of the oil on the uncalendered, hydrophobic substrate may be due to the lower coating coverage.

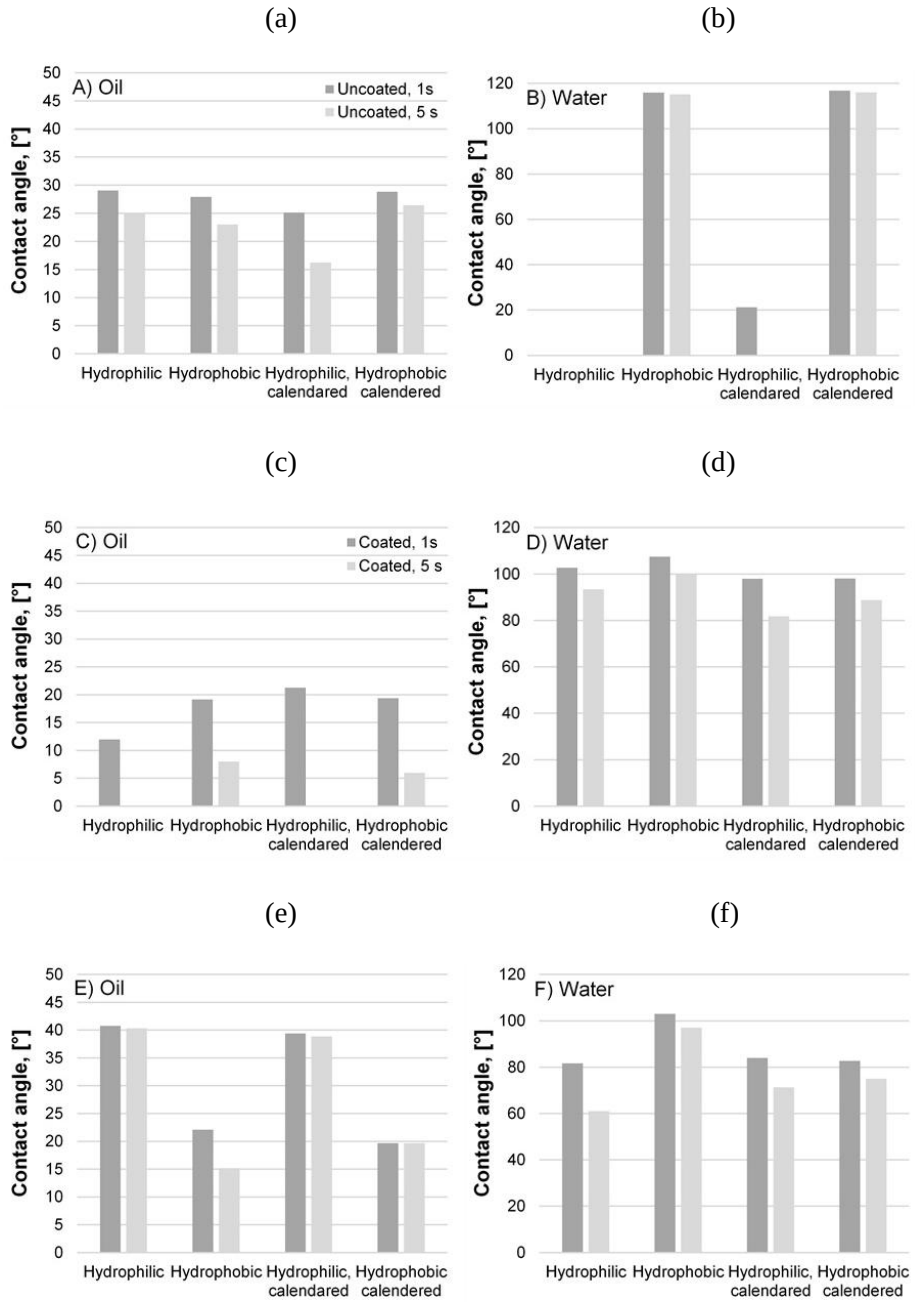

Figure 7.16: (a-b) Contact angles of oil and water on uncoated paper substrates and on (c-d) EHEC-MFC and (e-f) methyl nanocellulose foam-coated surfaces after one second and after 5 seconds.

7.3.2 Oxygen transmission rate of the cast films

Table 7.2 shows the oxygen transmission rate (OTR) measured on the cast films (Paper II). The OTR of the MFC films was significantly affected by the drying temperature, since the OTR was significantly higher when the film was dried at an elevated temperature. Similar high OTR values for films dried at elevated temperature have been reported for the same MFC grade by Padberg et al. (2016). The addition of MFC reduced the OTR of the EHEC-MFC and methyl nanocellulose-MFC films dried at 50 °C and the OTR of the EHEC-methyl nanocellulose films decreased with increasing addition of methyl nanocellulose but the decrease was not as great as with other compositions. It seems that in the preparation of films of MFC and hydrophobically modified EHEC or methyl nanocellulose, the addition of hydrophobically modified EHEC or methyl nanocellulose improve the film forming and thus provide a better oxygen barrier.

At the elevated temperature, air bubbles were formed in certain compositions, especially in the EHEC-MFC films with a ratio of 25:75. Despite the air bubbles (Figure 7.9), the film was uniform and provided the greatest oxygen barrier and the air bubbles thus did not weaken the oxygen barrier of the film. Similar results were obtained with methyl nanocellulose-MFC film in the same ratio, in which bubbles were also formed. This confirms that the film-forming properties of hydrophobically modified EHEC and methyl nanocellulose play an important role since pure MFC films had the highest OTR when the films were dried at elevated temperatures.

The OTR of the EHEC-MFC films dried at a lower temperature was different from that of the films dried at an elevated temperature. A possible interaction between EHEC and MFC was indicated by the viscosity measurements since the viscosity at room temperature of the compositions in a ratio of 75:25 and 50:50 was lower, especially in a ratio of 50:50. At this ratio, the lowest OTR was obtained, when the films were dried at a lower temperature. It is possible that the amount of flocs is reduced in the solution at this ratio and this enables the formation of a more uniform film. The different compositions also indicated an interaction with a ratio of 25:75, which could explain the lowest OTR value of the film when compared to that of the pure films dried at an elevated temperature.

Table 7.2: The oxygen transmission rate (OTR) of the EHEC-MFC, EHEC-methyl nanocellulose and methyl nanocellulose-MFC films with a grammage of 30 g/m^2. The EHEC-MFC films were dried at 23 °C and 50 % RH and 50 °C. The EHEC-methyl nanocellulose and methyl nanocellulose-MFC films were dried at 50 °C. The test conditions for the OTR measurements were 23 °C and 50 % RH.

	Oxygen transmission rate, [ml/m^2·day]			
Drying temperature	23 °C	50 °C	50 °C	50 °C
Composition	EHEC:MFC		EHEC:methyl nanocellulose	Methyl nanocellulose:MFC
100:0	1150	942	942	435
75:25	350	366	741	201
50:50	72	164	604	93
25:75	229	81	321	41
0:100	20	1447	435	1447

7.3.3 **Oil and grease resistance**

Oil and grease resistance was measured from the cast films (Paper II) and blade-coated (Paper III) and foam-coated (Paper IV) substrates. The OGR of the cast films was determined by a modified method without placing a weight on the oil drop as is normally done according to the ISO 16532-1 standard. Cast films showed a high oil and grease resistance, since oil did not penetrate through the samples in 24 hours. Differences in oil spreading behaviour was observed between the different compositions, and this was also observed in the contact angle determinations with rapeseed oil (Figure 7.14).

The OGR of the foam-coated hydrophilic and hydrophobic substrates was measured according to the standard, but their oil and grease resistance was poor due to the insufficient coat weight and uneven coating coverage. On the hydrophobic substrates, a coat weight of 3.2 g/m^2 and lower were sufficient to lower the air permeance significantly and modify the surface depending on the coating composition, as indicated by the oil and water contact angle measurements. The spreading of oil varied also. The oil spread and was absorbed immediately by the EHEC-MFC coated samples, whereas oil penetrated through pinholes in the methyl nanocellulose coated samples.

Air permeance has been found to correlate with oil and grease resistance, and the OGR increases with decreasing air permeance (Kjellgren et al. 2006). The substrate used in non-foamed methyl nanocellulose-based coatings had an air permeance of 370 ml/min, and a coating with a non-foamed solution EHEC-MFC or MFC reduced the air permeance but did not give any oil or grease resistance due to the uneven coating coverage and inadequate coat weight (Paper III). All the methyl nanocellulose-containing coatings

reduced the air permeance significantly already after a single coating layer, indicating that a dense coating and good coverage was achieved with a low coat weight (Table 7.3). A coat weight over 4 g/m^2 was required to reduce the air permeance to 0 ml/min, but this was still not sufficient to provide a greaseproof coating. In the case of the methyl nanocellulose and methyl nanocellulose-MFC, the coating was found to be greaseproof at coat weights of 10 and 9 g/m^2 and with increasing thickness of the coating layer.

With methyl nanocellulose foam, a coat weight of 3 g/m^2 was achieved on calendered hydrophobic paper substrate after three coating layers, and the air permeance was then reduced by 99 % compared to that of the uncoated substrate. With a foam coating, the air permeance can be reduced already at a low coat weight, but the coating uniformity or the thickness of the coating layer were not sufficient to create an oil and grease barrier.

Table 7.3: The coat weight, thickness, oil and grease resistance, and air permeance of the methyl nanocellulose-based and MFC coatings and films. For OGR, the highest and lowest results are presented. 24 h refers to greaseproof material. Methyl nanocellulose-MFC and methyl nanocellulose-EHEC compositions were in a ratio of 90:10. The base paper was used in the foam coating. (Adapted from Papers II, III and IV).

	Coat weight, [g/m^2]	Coating thickness, [µm]	OGR, [min]	$OGR_{rapeseed\ oil}$, [min]	Air permeance, [ml/min]
Base paper			-	-	198
Base board			-	-	370
Methyl nanocellulose					
Foam coating	3.0	n.m.	-	-	1
Coating	4.3	1	2/2	8/10	0.5
Coating	7.5	6	120/120	60/60	0
Coating	10.0	9	360/24 h	120/120	0
Film	30.0	n.m.	24 h	n.m.	n.m.
Methyl nanocellulose-MFC					
Coating	2.0	-	-	2/3	16
Coating	4.5	7	20/120	30/60	0
Coating	9.0	7	360/24 h	120/120	0
Methyl nanocellulose-EHEC					
Coating	1.5	4	-	2/3	27
Coating	4.0	7	9/20	8/10	0
Coating	7.0	19	20/30	10/25	0
MFC					
Coating	5.0	26	-	-	210
Film	30.0	n.m.	24 h	n.m.	n.m.

The differences between the highest and lowest OGR values measured on the same sample, however, indicate pinholes in the coating (Paper III). The addition of MFC to the methyl nanocellulose coating led to a longer OGR time at a similar coat weight than the methyl nanocellulose coating, possibly due to an increase in the tortuosity of the coating (Ovaska et al. 2015) and an increase in coating layer thickness. This was also noticed when the OGR was measured on the methyl nanocellulose coated samples, where the air permeance was 0 ml/min on three- and five-times coated samples and the thickness was greater, which improved the oil and grease resistance of the material (Figure 7.17). To

achieve OGR of 20 minutes, at least 4 g/m^2 and a 6 µm thick coating and an air permeance of 0 ml/min were required. This meant that, the thickness of the EHEC-methyl nanocellulose coating after five coating layers should give a good OGR value, but the presence of hydrophobically modified EHEC in the coating changed the behaviour of oil on the surface, and several defects were also found in the coating. The MFC coating should provide high OGR, but the coated samples did not repel the oil. The air permeance of the MFC coating was high, due to an uneven coating coverage as shown by the SEM - images (Figure 7.10).

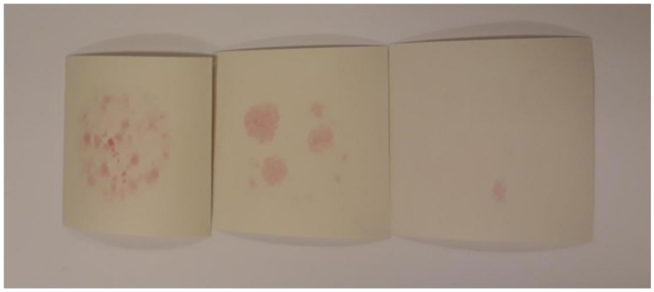

Figure 7.17: The penetration of oil through the methyl nanocellulose-coated samples. The samples had one, three or five coating layers (from the left) with an oil and grease resistance of 2 minutes, 25 minutes and 6 hours, respectively.

The OGR of the methyl nanocellulose-based coatings was also measured at 23 °C and 50 % RH using rapeseed oil (Table 7.3) (Paper III). In the case of the methyl nanocellulose-EHEC coating, the penetration of the oil was not significantly different from that of the oil used in the standard. At lower coat weights, the OGR of the methyl nanocellulose and methyl nanocellulose-MFC coatings was slightly larger with rapeseed oil, but at higher coat weights, the OGR was less than with the standard oil.

The methyl nanocellulose and methyl nanocellulose-MFC coatings showed a high OGR value but in some cases, oil penetrated through pinholes. SEM images of the five-times coated samples confirmed that the penetration of oil through the material was due to pinhole or crack rather than to a wetting and dissolution of the material (Figure 7.18). The pinholes are seen as dark areas in the coating due to the penetration of rapeseed oil. A visual examination indicated that in all cases the oil penetrated through a pinhole, as in the case of the methyl nanocellulose coating (Figure 7.18(a)). Figure 7.18(b) shows that in the case of the methyl nanocellulose-MFC coating, two pinholes were observed close to each other and oil may have penetrated through both pinholes. In the case of methyl nanocellulose-EHEC coating (Figure 7.18(c)), SEM-images revealed cracks in the coating where the oil had penetrated. These cracks are probably due to shrinkage of the coating during drying which reaches all the coating layers leading to poor oil and grease resistance.

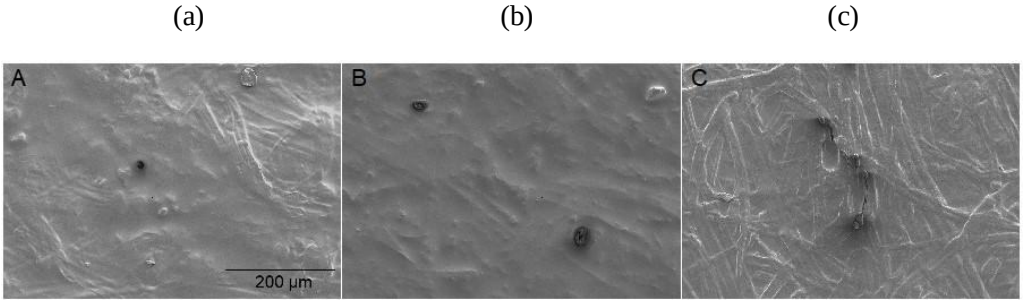

Figure 7.18: The penetration of rapeseed oil through defects in (a) methyl nanocellulose, (b) methyl nanocellulose-MFC, and (c) methyl nanocellulose-EHEC coatings.

Post-treatments, conditioning at 70 % relative humidity or drying at 105 °C, were performed on the methyl nanocellulose-based coatings and their effects on oil and grease resistance are shown in Table 7.4 (Paper III). Prior to the OGR measurements, the coated samples were conditioned at 70 % RH. Conditioning at a high relative humidity weakened the oil and grease barrier provided by the methyl nanocellulose, especially in the case of the methyl nanocellulose-MFC coating probably due to a weakening of the MFC network at high relative humidity. In the case of the methyl nanocellulose-EHEC coating, the conditioning did not weaken the OGR. The hydrophobicity of EHEC in the coating may be beneficial if the material is exposed to a high relative humidity.

Post-drying of the coated samples was conducted at 105 °C, and the OGR of the post-dried samples was determined after conditioning at 23 °C and 50 % RH. Post-drying did not reduce the OGR of methyl nanocellulose coating, but the OGR of methyl nanocellulose-MFC and methyl nanocellulose-EHEC decreased after post-drying. This weakening of the OGR may be due to defects which developed in the coating by shrinkage during drying. In the methyl nanocellulose-EHEC coating, some cracks were observed already before the post-drying, and the post-drying may have led to the further formation of defects.

Table 7.4: Oil and grease resistance (OGR) of the uncoated and coated samples measured at 60 °C (adapted from Paper III).

	Oil and grease resistance, [min]	
	Conditioning 70 % RH	Post-drying 105 °C
	Min/max	Min/max
Uncoated	-	-
Methyl nanocellulose		
x1	-	1/1
x3	30/120	30/180
x5	240/240	360/Greaseproof
Methyl nanocellulose-MFC		
x1	-	-/1
x3	2/4	9/30
x5	180	120/120
Methyl nanocellulose-EHEC		
x1	-	-/1
x3	25/30	1/3
x5	30/40	3/4

7.3.4 Mechanical durability of the coatings

Creasing and folding tests were carried out on the methyl nanocellulose, methyl nanocellulose-MFC and methyl nanocellulose-EHEC coated samples (Paper III). The coatings consisted of five coating layers. Creasing and folding were conducted in order to study the effect of subsequent converting processes on the oil and grease resistance of the material and the ability of the material to withstand creasing and folding.

The OGR was measured on samples that had been creased and folded in both cross and machine directions. The oil was then applied on the intersection of the folds. Creasing and folding of the materials affected the coating and its barrier properties, since oil penetrated through the folded area and the OGR was reduced in all the samples.

SEM images of the folded areas revealed that folding caused cracks in the methyl nanocellulose coating which are seen in the Figure 7.19(a), but no defects were observed in the methyl nanocellulose-MFC coating (Figure 7.19(b)). The surface nevertheless seemed denser, and the lower OGR value indicated either nanoscale defects or that the lower coating layers were weakened by the folding. The addition of MFC to the coating composition seemed to increase the ability of the coating to resist or withstand the stresses occurring during folding. Figure 7.19(c) shows spherical defects in methyl nanocellulose-EHEC coating due to the coating process. In addition, in the methyl nanocellulose-EHEC

coating cracks were observed in the coating after drying indicating a more brittle coating compared to the methyl nanocellulose-containing coatings.

(a) (b) (c)

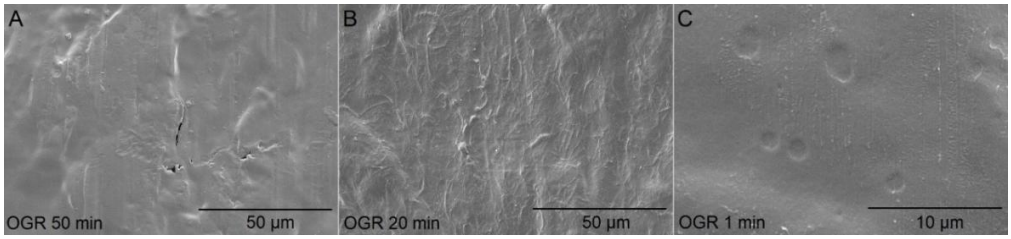

Figure 7.19: The effect of creasing and folding on five-times coated (a) methyl nanocellulose, (b) methyl nanocellulose-MFC and (c) methyl nanocellulose-EHEC coatings, with an oil and grease resistance of 50 min, 20 min and 1 min, respectively.

8 Conclusions

In this study, the interaction and thermoresponsive properties of methyl nanocellulose, hydrophobically modified EHEC and MFC have been investigated with rheological measurements and their effects in the film formation has been evaluated. The barrier properties of the methyl nanocellulose-based films and coatings with different proportions of hydrophobically modified EHEC or MFC were investigated. Coatings were made with non-foamed and foamed solutions on paper and paperboard substrates. The barrier properties of the films and coatings were evaluated with oil and grease resistance and oxygen transmission rate measurements.

The EHEC-methyl nanocellulose, EHEC-MFC and methyl nanocellulose-MFC solutions showed interactions at certain compositions which was seen as changes in the initial viscosity, gelation temperature or cloud point temperature. When cast films were prepared, the pure EHEC and methyl nanocellulose films were transparent, but the mixtures of the components gave less transparent films. In addition, the possible interaction between the components was found to affect the oxygen transmission rate of the cast films dried at room temperature. In the case of the EHEC-MFC and methyl nanocellulose-MFC films, a certain composition influenced the stabilization of the air bubbles in the cast films when the films were dried at elevated temperature, but the bubbles did not weaken the barrier properties. In general, the oxygen barrier was affected by the drying temperature and the composition of the films, showing significant differences between the films containing native MFC, hydrophobically modified EHEC or methyl nanocellulose.

The oil and grease resistance was over 24 hours for all the cast films, but the spreading of the oil differed significantly between the samples. Similar spreading effect was found on the coatings made with non-foamed and foamed solutions. Methyl nanocellulose-containing films increased the oil repellence and EHEC-MFC films increased the hydrophobicity of the surface. These results, together with the OTR results, suggest that the interaction between the components in the aqueous phase has a stronger impact on the OTR value than on the OGR value.

Different compositions were investigated in coating applications, showing that the coating uniformity and thickness were found to have a great impact on the barrier results. Methyl nanocellulose and methyl nanocellulose-MFC coatings could be utilized to create a strong oil and grease barrier. The addition of MFC to the coating increases the thickness and tortuosity, which have a positive effect on the oil and grease barrier, but it seemed also to increase the material’s ability to withstand the stresses to which the material is subjected in converting. The addition of hydrophobically modified EHEC to the coating increases the spreading and absorption of oil, but it does not necessarily result in a weakening of the grease barrier.

Foam can be utilized to create thin coatings in order to modify the surface. Foam containing hydrophobically modified EHEC created a highly hydrophobic surface,

whereas methyl nanocellulose was able to increase the oil repellence already at low coat weights. It was also found that the stability of the foam and the foam-substrate interaction have a great effect on the coating quality and that foam coating can also be utilized to create an oil and grease barrier with methyl nanocellulose.

References

Andersen, M., Johansson, L.-S., Tanem, B. S., Stenius, P. (2006). Properties and characterization of hydrophobized microfibrillated cellulose. *Cellulose*, 13(6), pp. 665-677.

Anderson, T. E. (1977). *Use of foam in surface treatment of paper*, Patent US4597831A.

Andersson, C. (2008). New ways to enhance the functionality of paperboard by surface treatment – a review. *Packaging Technology and Science*, 21(6), pp. 339-373.

Arvidson, S. A., Lott, J. R., McAllister, J. W., Zhang, J., Bates, F. S., Lodge, T. P., Sammler, R. L., Li, Y., Brackhagen, M. (2013). Interplay of phase separation and thermoreversible gelation in aqueous methylcellulose solutions. *Macromolecules*, 46(1), pp. 300-309.

Aulin, C., Gällstedt, M., Lindström, T. (2010). Oxygen and oil barrier properties of microfibrillated cellulose films and coatings. *Cellulose*, 17(3), pp. 559-574.

Baez, C., Considine, J., Rowlands, R. (2014). Influence of drying restraint on physical and mechanical properties of nanofibrillated cellulose films, *Cellulose*, 21(1), pp. 347-356.

Beex, L. A. A. and Peerlings, R. H. J. (2009). An experimental and computational study of laminated paperboard creasing and folding. *International Journal of Solid Structures*, 46(24), pp. 4192-4207.

Bilbao-Sainz, C., Bras, J., Williams, T., Sénechal, T., Orts, W. (2011). HPMC reinforced with different cellulose nanoparticles. *Carbohydrate Polymers*, 86, pp. 1549-1557.

Boissard, Y. (2017). MFC for paper surface treatment. Luleå University of Technology, Sweden.

Carlsson, A., Karlström, G., Lindman, B. (1986). Synergistic surfactant-electrolyte effect in polymer solutions. *Langmuir*, 2(4), pp. 536-537.

Cervin, N. T., Andersson, L., Ng, J. B. S., Olin, P., Bergström, L., Wågberg, L. (2013). Lightweight and strong cellulose materials made from aqueous foams stabilized by nanofibrillated cellulose. *Biomacromolecules*, 14(2), pp. 503-511.

Cervin, N. T., Johansson, E., Benjamins, J.-W., Wågberg, L. (2015). Mechanisms behind the stabilizing action of cellulose nanofibrils in wet-stable cellulose foams. *Biomacromolecules*, 16(3), pp. 822-831.

Cervin, N. T, Johansson, E., Larsson, P. A, Wågberg, L. (2016). Strong, water-durable, and wet-resilient cellulose nanofibril-stabilized foams from oven drying. *ACS Applied Materials & Interfaces*, 8(18), pp. 11682-11689.

Cheng, C. J. and Jones, O. G. (2019). Effect of drying temperature and extent of particle dispersion on composite films of methyl cellulose and zein nanoparticles. *Journal of Food Engineering*, 250, pp. 26-32.

Ciftci, G. C., Larsson, P. A., Riazanova, A. V., Øvrebø, H. H., Wågberg, L., Berglund, L. A. (2020). Tailoring of rheological properties and structural polydispersity effects in microfibrillated cellulose suspensions. *Cellulose*, 27(16), pp. 9227-9241.

Cozzolino, C. A., Cerri, G., Brundu, A., Farris, S. (2014). Microfibrillated cellulose (MFC): pullulan bionanocomposite films. *Cellulose*, 21(6), pp. 4323-4335.

Debeaufort, F., Quezada-Gallo J. A., Delporte, B., Voilley, A. (2000). Lipid hydrophobicity and physical state effects on the properties of bilayer edible films. *Journal of Membrane Science*, 180(1), pp. 47-55.

D'Eon, J. C., Crozier, P. W., Furdui, V. I., Reiner, E. J., Libelo, E. L., Mabury, S. A. (2009). Observation of a commercial fluorinated material, the polyfluoroalkyl phosphoric acid diesters, in human sera, wastewater treatment plant sludge, and paper fibers. *Environmental Science & Technology*, 43(12), pp. 4589-4594.

Eronen, P., Junka, K., Laine, J., Österberg, M. (2011). Interaction between water soluble polysaccharides and native nanofibrillar cellulose thin films. *BioResources*, 6(4), pp. 4200-4217.

European Commission. Commission Regulation (EU) 2017/1000 Annex XVII to Regulation (EC) No 1907/2006 of the European Parliament and of the Council concerning the Registration, Evaluation, Authorisation and Restriction of Chemicals (REACH) as regards perfluorooctanoic acid (PFOA), its salts and PFOA-related substances.

Fairclough, J. P. A., Yu, H., Kelly, O., Ryan, A. J., Sammler, R. L., Radler, M. (2012). Interplay between gelation and phase separation in aqueous solutions of methylcellulose and hydroxypropylmethylcellulose. *Langmuir*, 28(28), pp. 10551-10557.

Fein, K., Bousfield, D. W., Gramlich, W. M. (2020). The influence of versatile thiol-norbornene modifications to cellulose nanofibers on rheology and film properties. *Carbohydrate Polymers*, 230, 115672.

Ferrer, A., Pal, L., Hubbe, M. (2017). Nanocellulose in packaging: Advances in barrier layer technologies. *Industrial Crops and Products*, 95, pp. 574-582.

Fujisawa, S., Togawa, E., Kuroda, K. (2017). Nanocellulose-stabilized Pickering emulsions and their applications. *Science and Technology of Advanced Materials*, 18(1), pp. 959-971.

Fukuzumi, H., Saito, T., Iwata, T., Kumamoto, Y., Isogai, A. (2009). Transparent and high gas barrier films of cellulose nanofibers prepared by TEMPO-mediated oxidation. *Biomacromolecules*, 10(1), pp. 162-165.

George, J., Kumar, R., Sajeevkumar, V. A., Ramana, K. V., Rajamanickam, R., Abhishek, V., Nadanasabapathy, S., Siddaramaiah. (2014). Hybrid HPMC nanocomposites containing bacterial nanocrystals and silver nanoparticles. *Carbohydrate Polymers*, 105, pp. 285-292.

Gong, X., Wang, Y., Chen, L. (2017). Enhanced emulsifying properties of wood-based cellulosenanocrystals as Pickering emulsion stabilizer. *Carbohydrate Polymers*, 169, pp. 295-303.

Gordeyeva, K. S., Fall, A. B., Hall, S., Wicklein, B., Bergström, L. (2016). Stabilizing nanocellulose-nonionic surfactant composite foams by delayed Ca-induced gelation. *Journal of Colloid and Interface Science*, 472, pp. 44-51.

Guérin D. (2019). Wet lamination of micro-fibrillated celluloses, a new concept for paper surface treatment. *Specialty Papers Europe*, 9-10 April 2019, Berlin, Germany.

Hansen, N. M. L., Blomfeldt, T. O. J., Hedenqvist, M. S., Plackett, D. V. (2012). Properties of plasticized composite films prepared from nanofibrillated cellulose and birch wood xylan. *Cellulose*, 19(6), pp. 2015-2031.

Hejda, F., Solař, P., Kousal, J. (2010). Surface free energy determination by contact angle measurements - A comparison of various approaches. *WDS'10 Proceedings of Contributed Papers, Part III*, pp. 25-30.

Helanto, K., Matikainen, L., Talja, R., Rojas, O. J. (2019). Bio-based polymers for sustainable packaging and biobarriers: A critical review. *BioResources*, 14(2), pp. 4902-4951.

Herrera, M. A., Mathew, A. P., Oksman, K. (2017). Barrier and mechanical properties of plasticized and cross-linked nanocellulose coatings for paper packaging applications. *Cellulose*, 24(9), pp. 3969-3980.

Hiltunen, S., Heiskanen, I., Backfolk, K. (2018). Effect of hydrothermal treatment of microfibrillated cellulose on rheological properties and formation of hydrolysis products. *Cellulose*, 25(8), pp. 4653-4662.

Hu, Z., Xu, R., Cranston, E. D., Pelton, R. H. (2016). Stable aqueous foams from cellulose nanocrystals and methyl cellulose. *Biomacromolecules*, 17, pp. 4095-4099.

Hubbe, M. A., Ferrer, A., Tyagi, P., Yin, Y., Salas, C., Pal, L., and Rojas, O. J. (2017). Nanocellulose in thin films, coatings, and plies for packaging applications: A review. *BioResources*, 12(1), pp. 2143-2233.

Hubbe, M. A. and Pruszynski, P. (2020). Greaseproof paper products: A review emphasizing ecofriendly approaches. *BioResources*, 15(1), pp. 1978-2004.

Hult, E., Iotti, M., Lenes, M. (2010). Efficient approach to high barrier packaging using microfibrillar cellulose and shellac. *Cellulose*, 17(3), pp. 575-586.

Innotech Materials. Methyl nanocellulose. [Retrieved: May 4, 2020], url: http://www.innotechmaterials.com/methyl-nanocellulose.

Iotti, M., Gregersen, Ø. W., Moe, S., Lenes, M. (2011). Rheological studies of microfibrillar cellulose water dispersions. *Journal of Polymers and the Environment*, 19(1), pp. 137-145.

Isogai, A., Saito, T., Fukuzumi, H. (2011). TEMPO-oxidized cellulose nanofibers. *Royal Society of Chemistry*, 3, pp. 71-85.

Jain, S., Sandhu, P. S., Malvi, R., Gupta, B. (2013). Cellulose derivatives as thermoresponsive polymer: An overview. *Journal of Applied Pharmaceutical Science*, 3(12), pp. 139-144.

Jin, W. (2017). *Preparation of modified cellulose and its derivatives.* Patent WO2017075417A1.

Kamitakahara, H., Yoshinaga, A., Aono, H., Nakatsubo, F., Klemm, D., Burchard, W. (2008). New approach to unravel the structure-property relationship on methylcellulose, self-assembly of amphiphilic block-like methylated cello-oligosaccharides. *Cellulose*, 15(6), pp. 797-801.

Karlson, L., Joabsson, F., Thuresson K. (2000). Phase behavior and rheology in water and in model paint formulations thickened with HM-EHEC: influence of the chemical structure and the distribution of hydrophobic tails. *Carbohydrate Polymers*, 41, pp. 25-35.

Karppinen, A., Saarinen, T., Salmela, J., Laukkanen, A., Nuopponen, M., Seppälä, J. (2012). Flocculation of microfibrillated cellulose in shear flow. *Cellulose*, 19(6), pp. 1807-1819.

Kenttä, E., Kinnunen-Raudaskoski, K., Hjelt, T. (2014). Characterization of thin pigment coating layers produced by foam coating. *TAPPI Journal*, 13(7), p. 21-27.

Khalifa, Y. I. M. (2016). Effect of the printing remedies and lamination techniques on barrier properties "WVTR and OTR value" for polypropylene film. *EC Nutrition*, 5(2), pp. 1089-1099.

Khan, A. R, Salmieri, S., Dussault, D., Uribe-Calderon, J., Kamal. M. R, Safrany, A., Lacroix, M. (2010). Production and properties of nanocellulose-reinforced methylcellulose-based biodegradable films. *Journal of Agricultural and Food Chemistry*, 58, pp. 7878-7885.

Khuman, P., Singh W. B. K, Dushila, S. D., Naorem, H. (2014). Viscosity-temperature behavior of hydroxypropyl cellulose solution in presence of an electrolyte or a surfactant: a convenient method to determine the cloud point of polymer solutions. *Journal of Macromolecular Science Part A: Pure and Applied Chemistry*, 51(11), pp. 924-930.

Kinnunen-Raudaskoski, K., Hjelt, T., Kenttä, E., Forsström, U. (2014). Thin coating for paper by foam coating. *TAPPI Journal*, 13(7), pp. 9-19.

Kinnunen-Raudaskoski, K., Hjelt, T., Forsström, U., Sadocco, P., Paltakari, J. (2017). Novel thin functional coatings for paper by foam coating. *TAPPI Journal*, 16(4), p. 179-186.

Kisonen, V., Xu, C., Bollström, R., Hartman, J., Rautkoski, H., Nurmi, M., Hemming, J., Eklund, P., Willför, S. (2014). O-acetyl galactoglucomannan esters for barrier coatings. *Cellulose*, 21(6), pp. 4497-4509.

Kjellgren, H., Gällstedt, M., Engström, G., Järnström, L. (2006). Barrier and surface properties of chitosan-coated greaseproof paper. *Carbohydrate Polymers*, 65(4), pp. 453-460.

Kjøniksen, A.-L., Nyström, B., Lindman, B. (1998). Dynamic viscoelasticity of gelling and nongelling aqueous mixtures of ethyl(hydroxyethyl)cellulose and an ionic surfactant. *Macromolecules*, 31(6), pp. 1852-1858.

Koponen, A., Jäsberg, A., Lappalainen, T., Kiiskinen, H. (2018). The effect of in-line foam generation on foam quality and sheet formation in foam forming. *Nordic Pulp & Paper Research Journal*, 33(3), p. 482-495

Koppolu R, Lahti J, Abitbol T, Swerin A, Kuusipalo J, Toivakka, M. (2019). Continuous processing of nanocellulose and polylactic acid into multilayer barrier coatings. *ACS Applied Materials & Interfaces*, 11, pp. 11920-11927.

Korehei, R., Jahangiri, P., Nikbakht, A., Martinez, M., Olson, J. (2016). Effects of drying strategies and microfibrillated cellulose fiber content on the properties of foam-formed paper. *Journal of Wood Chemistry and Technology*, 36(4), pp. 235-249.

Kronberg, B., Holmberg, K., Lindman, B. (2014). *Surface Chemistry of Surfactants and Polymers*. United Kingdom: John Wiley & Sons, Ltd. 479 p.

Kumar, V., Bollström, R., Yang, A., Chen, Q., Chen, G., Salminen, P., Bousfield, D., Toivakka, M. (2014). Comparison of nano- and microfibrillated cellulose films. *Cellulose*, 21(5), pp. 3443-3456.

Kumar, V., Elfving, A., Koivula, H., Bousfield, D., Toivakka, M. (2016). Roll-to-roll processed cellulose nanofiber coatings. *Industrial & Engineering Chemistry Research*, 55, pp. 3603-3613.

Kumar, V., Koppolu, V. R., Bousfield, D., Toivakka, M. (2017a). Substrate role in coating of microfibrillated cellulose suspensions. *Cellulose*, 24(3), pp. 1247-1260.

Kumar, V., Ottesen, V., Gregersen, Ø. W., Syverud, K., Toivakka, M. (2017b). Coatability of cellulose nanofibril suspensions – role of rheology and water retention. *BioResources*, 12(4), pp. 7656-7679.

Lam, S., Velikov, K. P., Velev, O. D. (2014). Pickering stabilization of foams and emulsions with particles of biological origin. *Current Opinion in Colloid & Interface Science*, 19, pp. 490-500.

Larsson, M., Hjärtstam, J., Larsson, A. (2012). Novel nanostructured microfibrillated cellulose–hydroxypropyl methylcellulose films with large one-dimensional swelling and tunable permeability. *Carbohydrate Polymers*, 88, pp. 763-771.

Lavoine, N., Desloges, I., Dufresne, A., Bras, J. (2012). Microfibrillated cellulose – Its barrier properties and applications in cellulosic materials: A review. *Carbohydrate Polymers*, 90(2), pp. 735-764.

Lavoine, N., Bras, J., Desloges, I. (2013). Mechanical and barrier properties of cardboard and 3D packaging coated with microfibrillated cellulose. *Journal of Applied Polymer Science*, 131(8), 40106.

Lavoine, N., Desloges, I., Khelifi, B., Bras, J. (2014). Impact of different coating processes of microfibrillated cellulose on the mechanical and barrier properties of paper. *Journal of Materials Science*, 49, pp. 2879-2893.

Lavoine, N. and Bergström, L. (2017). Nanocellulose-based foams and aerogels: processing, properties, and applications. *Journal of Materials Chemistry A*, 5, pp. 16105-16117.

Li, L., Breedveld, V., Hess, D. W. (2013). Design and fabrication of superamphiphobic paper surfaces. *ACS Applied Materials & Interfaces*, 5(11), pp. 5381-5386.

Li, J., Yang, X., Xiu, H., Dong, H., Song, T., Ma, F., Feng, P., Zhang, X., Kozliak, E., Ji, Y. (2019). Structure and performance of plant fiber based foam material by fibrillation via refining treatment. *Industrial Crops & Products*, 128, pp. 186-193.

Lindman, B., Karlström, G., Stigsson, L. (2010). On the mechanism of dissolution of cellulose. *Journal of Molecular Liquids*, 156(1), pp. 76-81.

Liu, Y., Kong, S., Xiao, H., Bai, C. Y., Lu, P., Wang, S. F. (2018). Comparative study of ultra-lightweight pulp foams obtained from various fibers and reinforced by MFC. *Carbohydrate Polymers* 182, pp. 92-97.

McKee, J. R., Hietala, S., Seitsonen, J., Laine, J., Kontturi, E., Ikkala, O. (2014). Thermoresponsive nanocellulose hydrogels with tunable mechanical properties. *ACS Macro Letters*, 3(3), pp. 266-270.

Minelli, M., Baschetti, M. G., Doghieri, F., Ankerfors, M., Lindström, T., Siró, I., Plackett, D. (2010). Investigation of mass transport properties of microfibrillated cellulose (MFC) films. *Journal of Membrane Science*, 358, pp. 67-75.

Mousavi, S. M. M., Afra, E., Tajvidi, M., Bousfield, D. W., Dehghani-Firouzabadi, M. (2018). Application of cellulose nanofibril (CNF) as coating on paperboard at moderate solids content and high coating speed using blade coater. *Progress in Organic Coatings*, 122, pp. 207-218.

Nair, S. S., Zhu, J. Y., Deng, Y., Ragauskas, AJ. (2014). High performance green barriers based on nanocellulose. *Sustainable Chemical Processes*, 2(23).

Nasatto, P. L., Pignon, F., Silveira, J. L. M., Duarte, M. E. R., Noseda, M. D., Rinaudo, M. (2015). Methylcellulose, a cellulose derivative with original physical properties and extended applications. *Polymers*, 7, pp. 777-803.

Nilsson, S., Thuresson, K., Lindman, B., Nyström, B. (2000). Associations in mixtures of hydrophobically modified polymer and surfactant in dilute and semidilute aqueous solutions. A rheology and PFG NMR self-diffusion investigation. *Macromolecules*, 33, pp. 9641-9649.

Nogi, M., Iwamoto, S., Nakagaito, A. N., Yano, H. (2009). Optically transparent nanofiber paper. *Advanced Materials*, 21(6), pp. 1595-1598.

Nyström, B., Thuresson, K., Lindman, B. (1995). Rheological and dynamic light-scattering studies on aqueous solutions of a hydrophobically modified nonionic cellulose ether and its unmodified analogue. *Langmuir*, 11(6), pp. 1994-2002.

Nyström, B., Kjøniksen, A. L., Lindman, B. (1996). Effects of temperature, surfactant, and salt on the rheological behavior in semidilute aqueous systems of a nonionic cellulose ether. *Langmuir*, 12(13), pp. 3233-3240.

Oinonen, P., Krawczyk, H., Ek, M., Henriksson, G., Moriana, R. (2016). Bioinspired composites from cross-linked galactoglucomannan and microfibrillated cellulose: Thermal, mechanical and oxygen barrier properties. *Carbohydrate polymers*, 136, pp.146-153.

Olafsson, G. and Hildingsson, I. (1995). Sorption of fatty acids into low-density polyethylene and its effects on adhesion with aluminum foil laminated packaging material. *Journal of Agricultural and Food Chemistry*, 43(2), pp. 306-312.

Olsson, M., Boström, G., Karlson, L., Piculell, L. (2005). Added surfactant can change the phase behavior of aqueous polymer-particle mixtures. *Langmuir*, 21(7), pp. 2743-2749

Osong, S. H., Norgren, S., Engstrand, P. (2016). Processing of wood-based microfibrillated cellulose and nanofibrillated cellulose, and applications relating to papermaking: a review. *Cellulose*, 23(1), pp. 93-123.

Oun, A. A. and Rhim, J. W. (2015). Preparation and characterization of sodium carboxymethyl cellulose/cotton linter cellulose nanofibril composite films. *Carbohydrate Polymers*, 127, pp. 101-109.

Ovaska, S.-S., Geydt, P., Österberg, M., Johansson, L.-S., Backfolk, K. (2015). Heat-Induced changes in oil and grease resistant hydroxypropylated-starch-based barrier coatings. *Nordic Pulp & Paper Research Journal*, 30(3), pp. 488-496.

Padberg, J., Bauer, W., Gliese, T. (2016). The influence of fibrillation on the oxygen barrier properties of films from microfibrillated cellulose. *Nordic Pulp & Paper Research Journal*, 31(4), pp. 548-560.

Padberg, J., Bauer, W., Gliese, T. (2017). Measuring the oil and grease barrier properties of MFC coated paper using ultrasonic signal variation. *TAPPI International Conference on Nanotechnology for Renewable Materials.* 5-8 June 2017. Montreal, Quebec, Canada.

Pahimanolis, N., Salminen, A., Penttilä, P. A., Korhonen, J. T., Johansson, L.-S., Ruokolainen, J., Serimaa, R., Seppälä, J. (2013). Nanofibrillated cellulose/carboxymethyl cellulose composite with improved wet strength. *Cellulose*, 20(3), pp. 1459-1468.

Paunonen, S. (2013). Strength and barrier enhancements of cellophane and cellulose derivative films: A review. *BioResources*, 8(2), pp. 3098-3121.

Plackett, D., Anturi, H., Hedenqvist, M., Ankerfors, M., Gällstedt, M., Lindström, T., Siró, I. (2010). Physical properties and morphology of films prepared from microfibrillated cellulose and microfibrillated cellulose in combination with amylopectin. *Journal of Applied Polymer Science*, 117(6), pp. 3601-3609.

Pugh, R. J. (2016). *Bubble and Foam Chemistry*. United Kingdom: Cambridge University Press.

Pääkkö, M., Ankerfors, M., Kosonen, H., Nykänen, A., Ahola, S., Österberg, M., Ruokolainen, J., Larsson, P. T., Ikkala, O., Lindström, T. (2007). Enzymatic hydrolysis combined with mechanical shearing and high-pressure homogenization for nanoscale cellulose fibrils and strong gels. *Biomacromolecules*, 8(6), p. 1934-1941.

Rodionova, G., Lenes, M., Eriksen, Ø., Gregersen, Ø. (2011). Surface chemical modification of microfibrillated cellulose: improvement of barrier properties for packaging applications. *Cellulose*, 18(1), pp. 127-134.

Rodionova, G., Hoff, B., Lenes, M., Eriksen, Ø., Gregersen, Ø. (2013). Gas-phase esterification of microfibrillated cellulose (MFC) films. *Cellulose*, 20(3), pp. 1167-1174.

Saarikoski, E., Rissanen, M., Seppälä, J. (2015). Effect of rheological properties of dissolved cellulose/microfibrillated cellulose blend suspension on film forming. *Carbohydrate Polymers*, 119, pp. 62-70.

Salam, A., Lucia, L. A, Jameel, H. (2015). Fluorine-based surface decorated cellulose nanocrystals as potential hydrophobic and oleophobic materials. *Cellulose*, 22(1), pp. 397-406.

Salas, C., Nypelö, T., Rodriguez-Abreu, C., Carrillo, C., Rojas, O. J. (2014). Nanocellulose properties and applications in colloids and interfaces. *Current Opinion in Colloid & Interface Science*, 19, pp. 383-396.

Salmén, L. and Stevanic, J. S. (2018). Effect of drying conditions on cellulose microfibril aggregation and "hornification". *Cellulose*, 25(11), pp. 6333-6344.

Sanchez-Garcia, M. D. and Lagaron, J. M. (2010). On the use of plant cellulose nanowhiskers to enhance the barrier properties of polylactic acid. *Cellulose*, 17(5), pp. 987-1004.

Sehaqui, H., Zhou, Q., Berglund L. A. (2011). Nanostructured biocomposites of high toughness – A wood cellulose nanofiber network in ductile hydroxyethylcellulose matrix. *Soft Matter*, 7(16), pp. 7342-7350.

Sehaqui, H., Zhou, Q., Berglund L. A. (2013). Nanofibrillated cellulose for enhancement of strength in high-density paper structures. *Nordic Pulp & Paper Research Journal*, 28(2), pp. 182-189.

Sheng, J., Li, J., Zhao, L. (2019). Fabrication of grease resistant paper with non-fluorinated chemicals for food packaging. *Cellulose*, 26(10), pp. 6291-6302.

Siró, I. and Plackett, D. (2010). Microfibrillated cellulose and new nanocomposite materials: a review. *Cellulose*, 17(3), pp. 459-494.

Solala, I., Bordes, R., Larsson, A. (2018). Water vapor mass transport across nanofibrillated cellulose films: effect of surface hydrophobization. *Cellulose*, 25(1), pp. 347-356.

Spence, K. L., Venditti, R. A., Rojas, O. J., Pawlak, J. J., Hubbe, M. A. (2011). Water vapor barrier properties of coated and filled microfibrillated cellulose composite films. *BioResources*, 6(4), pp. 4370-4388.

Stevanic, J. S., Bergström, E. M., Gatenholm, P., Berglund, L., Salmén, L. (2012). Arabinoxylan/nanofibrillated cellulose composite films. *Journal of Materials Science*, 47, pp. 6724-6732.

Sundman, O. (2014). Adsorption of four non-ionic cellulose derivatives on cellulose model surfaces. *Cellulose*, 21(1), pp. 115-124.

Syverud, K., Stenius, P. (2009). Strength and barrier properties of MFC films. *Cellulose*, 16(1), pp. 75-85.

Tammelin, T., Abburi, R., Gestranius, M., Laine, C., Setälä, H., Österberg, M. (2015). Correlation between cellulose thin film and supramolecular structures and interactions with water. *Soft Matter*, 11, pp. 4273-4282.

Tanninen, P., Saukkonen, E., Leminen, V., Lindell, H., Backfolk, K. (2015). Adjusting the die cutting process and tools for biopolymer dispersion coated paperboards. *Nordic Pulp & Paper Research Journal*, 30(2), pp. 336-343.

Tayeb, A. H., Tajvidi, M., Bousfield, D. (2020). Paper-based oil barrier packaging using lignin-containing cellulose nanofibrils. *Molecules*, 25:1344.

Thuresson, K., Nyström, B., Wang, G., Lindman, B. (1995). Effect of Surfactant on Structural and thermodynamic properties of aqueous solutions of hydrophobically modified ethyl (hydroxyethyl)cellulose. *Langmuir*, 11(10), pp. 3730-3736.

Thuresson, K. and Lindman, B. (1997). Effect of hydrophobic modification of a nonionic cellulose derivative on the interaction with surfactants. Phase behavior and association. *The Journal of Physical Chemistry*, 101(33), pp. 6460-6468.

Tyagi, P., Lucia, L. A., Hubbe, M. A., Pal, L. (2019). Nanocellulose-based multilayer barrier coatings for gas, oil, and grease resistance. *Carbohydrate Polymers*, 206, pp. 281-288.

Vikman, M., Vartiainen, J., Tsitko, I., Korhonen, P. (2015). Biodegradability and compostability of nanofibrillar cellulose-based products. *Journal of Polymers and the Environment*, 23, pp. 206-215.

Vuoti, S., Talja, R., Johansson, L.-S., Heikkinen, H., Tammelin, T. (2013). Solvent impact on esterification and film formation ability of nanofibrillated cellulose. *Cellulose*, 20(5), pp. 2359-2370.

Wang, G., Lindell, K., Olofsson, G. (1997). On the thermal gelling of ethyl(hydroxyethyl)cellulose and sodium dodecyl sulfate. Phase behavior and temperature scanning calorimetric response. *Macromolecules*, 30, pp. 105-112.

Wang, Y., Wang, X., Xie, Y., Zhang, K. (2018). Functional nanomaterials through esterification of cellulose: a review of chemistry and application. *Cellulose*, 25(7), pp. 3703-3731.

Wei, Y., Cheng, F., Hou, G., Sun, S. (2008). Amphiphilic cellulose: Surface activity and aqueous self assembly into nano-sized polymeric micelles. *Reactive & Functional Polymers*, 68, pp. 981-989.

Winnik, M. A. and Yekta, A. (1997). Associative polymers in aqueous solution. *Current Opinion in Colloid & Interface Science*, 2, pp. 424-436.

Xhanari, K., Syverud, K., Chinga-Carrasco, G., Paso, K., Stenius, P. (2011). Reduction of water wettability of nanofibrillated cellulose by adsorption of cationic surfactants. *Cellulose*, 18(2), pp. 257-270.

Xiang, W., Preisig, N., Ketola, A., Tardy, B. L., Bai, L., Ketoja, J. A., Stubenrauch, C., Rojas, O. J. (2019). How cellulose nanofibrils affect bulk, surface, and foam properties of anionic surfactant solutions. *Biomacromolecules*, 20, pp. 4361-4369.

Xu, Y., Li, L., Zheng, P., Lam, YC., Hu, X. (2014). Controllable gelation of methylcellulose by a salt mixture. *Langmuir*, 20(15), pp. 6134-6138.

Zhang, W., Xiao, H., Qian, L. (2014). Enhanced water vapour barrier and grease resistance of paper bilayer-coated with chitosan and beeswax. *Carbohydrate Polymers*, 101(1), pp. 401-406.

Zhong, L., Ding, Y., Zhang, B., Wang, Z., Li, C., Fu, X., Huang, Q. (2019). Effect of octenylsuccinylation of oxidized cassava starch on grease resistance and waterproofing of food wrapping paper. *Starch*, 71(7-8).

Österberg, M., Vartiainen, J., Lucenius, J., Hippi, U., Seppälä, J., Serimaa, R., Laine, J. (2013). A fast method to produce strong NFC films as a platform for barrier and functional materials. *ACS Applied Materials & Interfaces*, 5(11), pp. 4640-4647

Publication I

Lyytikäinen, J., Laukala, T., and Backfolk, K.
Temperature-dependent interactions between hydrophobically modified ethyl(hydroxyethyl)cellulose and methyl nanocellulose

Reprinted with permission from
Cellulose
Vol. 26(12), pp. 7079-7087, 2019

Publication II

Lyytikäinen, J., Morits, M., Österberg, M., Heiskanen, I., and Backfolk, K.
Skin and bubble formation in films made of methyl nanocellulose, hydrophobically modified ethyl(hydroxyethyl)cellulose and microfibrillated cellulose

Reprinted with permission from
Cellulose
28(2), pp. 787-797, 2021

Publication III

Lyytikäinen, J., Ovaska, S.-S., Heiskanen, I., and Backfolk, K.
The role of MFC and hydrophobically modified ethyl(hydroxyethyl)cellulose in film formation and the barrier properties of methyl nanocellulose film

Reprinted with permission from
Nordic Pulp & Paper Research Journal

The final publication is available at:
https://doi.org/10.1515/npprj-2020-0099

Publication IV

Lyytikäinen, J., Ovaska, S.-S., Heiskanen, I., and Backfolk, K.
Film formation and foamability of cellulose derivatives: Influence of co-binders and substrate properties on coating holdout

Reprinted with permission from
BioResources
Vol 16(1), pp. 597-613, 2021

ACTA UNIVERSITATIS LAPPEENRANTAENSIS

917. VIRTANEN, TIINA. Real-time monitoring of membrane fouling caused by phenolic compounds. 2020. Diss.

918. AZZUNI, ABDELRAHMAN. Energy security evaluation for the present and the future on a global level. 2020. Diss.

919. NOKELAINEN, JOHANNES. Interplay of local moments and itinerant electrons. 2020. Diss.

920. HONKANEN, JARI. Control design issues in grid-connected single-phase converters, with the focus on power factor correction. 2020. Diss.

921. KEMPPINEN, JUHA. The development and implementation of the clinical decision support system for integrated mental and addiction care. 2020. Diss.

922. KORHONEN, SATU. The journeys of becoming ang being an international entrepreneur: A narrative inquiry of the "I" in international entrepreneurship. 2020. Diss.

923. SIRKIÄ, JUKKA. Leveraging digitalization opportunities to improve the business model. 2020. Diss.

924. SHEMYAKIN, VLADIMIR. Parameter estimation of large-scale chaotic systems. 2020. Diss.

925. AALTONEN, PÄIVI. Exploring novelty in the internationalization process - understanding disruptive events. 2020. Diss.

926. VADANA, IUSTIN. Internationalization of born-digital companies. 2020. Diss.

927. FARFAN OROZCO, FRANCISCO JAVIER. In-depth analysis of the global power infrastructure - Opportunities for sustainable evolution of the power sector. 2020. Diss.

928. KRAINOV, IGOR. Properties of exchange interactions in magnetic semiconductors. 2020. Diss.

929. KARPPANEN, JANNE. Assessing the applicability of low voltage direct current in electricity distribution - Key factors and design aspects. 2020. Diss.

930. NIEMINEN, HARRI. Power-to-methanol via membrane contactor-based CO2 capture and low-temperature chemical synthesis. 2020. Diss.

931. CALDERA, UPEKSHA. The role of renewable energy based seawater reverse osmosis (SWRO) in meeting the global water challenges in the decades to come. 2020. Diss.

932. KIVISTÖ, TIMO. Processes and tools to promote community benefits in public procurement. 2020. Diss.

933. NAQVI, BILAL. Towards aligning security and usability during the system development lifecycle. 2020. Diss.

934. XIN, YAN. Knowledge sharing and reuse in product-service systems with a product lifecycle perspective. 2020. Diss.

935. PALACIN SILVA, VICTORIA. Participation in digital citizen science. 2020. Diss.

936. PUOLAKKA, TIINA. Managing operations in professional organisations – interplay between professionals and managers in court workflow control. 2020. Diss.

937. AHOLA, ANTTI. Stress components and local effects in the fatigue strength assessment of fillet weld joints made of ultra-high-strength steels. 2020. Diss.

938. METSOLA, JAAKKO. Good for wealth or bad for health? Socioemotional wealth in the internationalisation process of family SMEs from a network perspective. 2020. Diss.

939. VELT, HANNES. Entrepreneurial ecosystems and born global start-ups. 2020. Diss.

940. JI, HAIBIAO. Study of key techniques in the vacuum vessel assembly for the future fusion reactor. 2020. Diss.

941. KAZARNIKOV, ALEXEY. Statistical parameter identification of reaction-diffusion systems by Turing patterns. 2020. Diss.

942. SORMUNEN, PETRI. Ecodesign of construction and demolition waste-derived thermoplastic composites. 2020. Diss.

943. MANKONEN, ALEKSI. Fluidized bed combustion and humidified gas turbines as thermal energy conversion processes of the future. 2020. Diss.

944. KIANI OSHTORJANI, MEHRAN. Real-time efficient computational approaches for hydraulic components and particulate energy systems. 2020. Diss.

945. PEKKANEN, TIIA-LOTTA. What constrains the sustainability of our day-to-day consumption? A multi-epistemological inquiry into culture and institutions. 2021. Diss.

946. NASIRI, MINA. Performance management in digital transformation: a sustainability performance approach. 2021. Diss.

947. BRESOLIN, BIANCA MARIA. Synthesis and performance of metal halide perovskites as new visible light photocatalysts. 2021. Diss.

948. PÖYHÖNEN, SANTERI. Variable-speed-drive-based monitoring and diagnostic methods for pump, compressor, and fan systems. 2021. Diss.

949. ZENG, HUABIN. Continuous electrochemical activation of peroxydisulfate mediated by single-electron shuttle. 2021. Diss.

950. SPRINGER, SEBASTIAN. Bayesian inference by informative Gaussian features of the data. 2021. Diss.

951. SOBOLEVA, EKATERINA. Microscopy investigation of the surface of some modern magnetic materials. 2021. Diss.

952. MOHAMMADI ASL, REZA. Improved state observers and robust controllers for non-linear systems with special emphasis on robotic manipulators and electro-hydraulic servo systems. 2021. Diss.

953. VIANNA NETO, MÁRCIO RIBEIRO. Synthesis and optimization of Kraft process evaporator plants. 2021. Diss.

954. MUJKIC, ZLATAN. Sustainable development and optimization of supply chains. 2021. Diss.

LUT University

ISBN 978-952-335-638-2
ISBN 978-952-335-639-9 (PDF)
ISSN-L 1456-4491
ISSN 1456-4491
Lappeenranta 2021